



**HOKKAIDO**  
UNIVERSITY

# Topology Optimization Based on Deep Learning and toward Their Coevolution

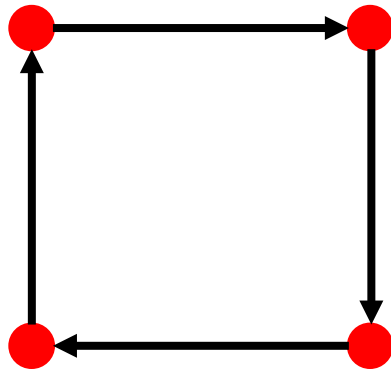
Presented at JSST2018, Muroran, September 18, 2018

**Hajime Igarashi**

Hokkaido University

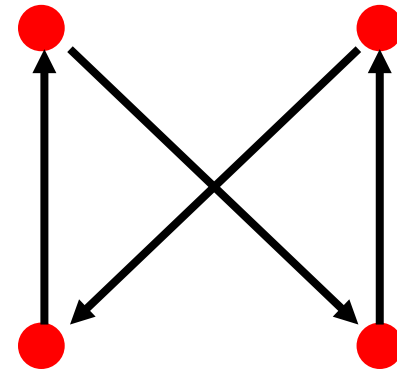
# Traveling Salesman Problem (TSP)

Given a list of cities and the distances between each pair of cities, what is the shortest possible route that visits each city and returns to the origin city? (Wiki)



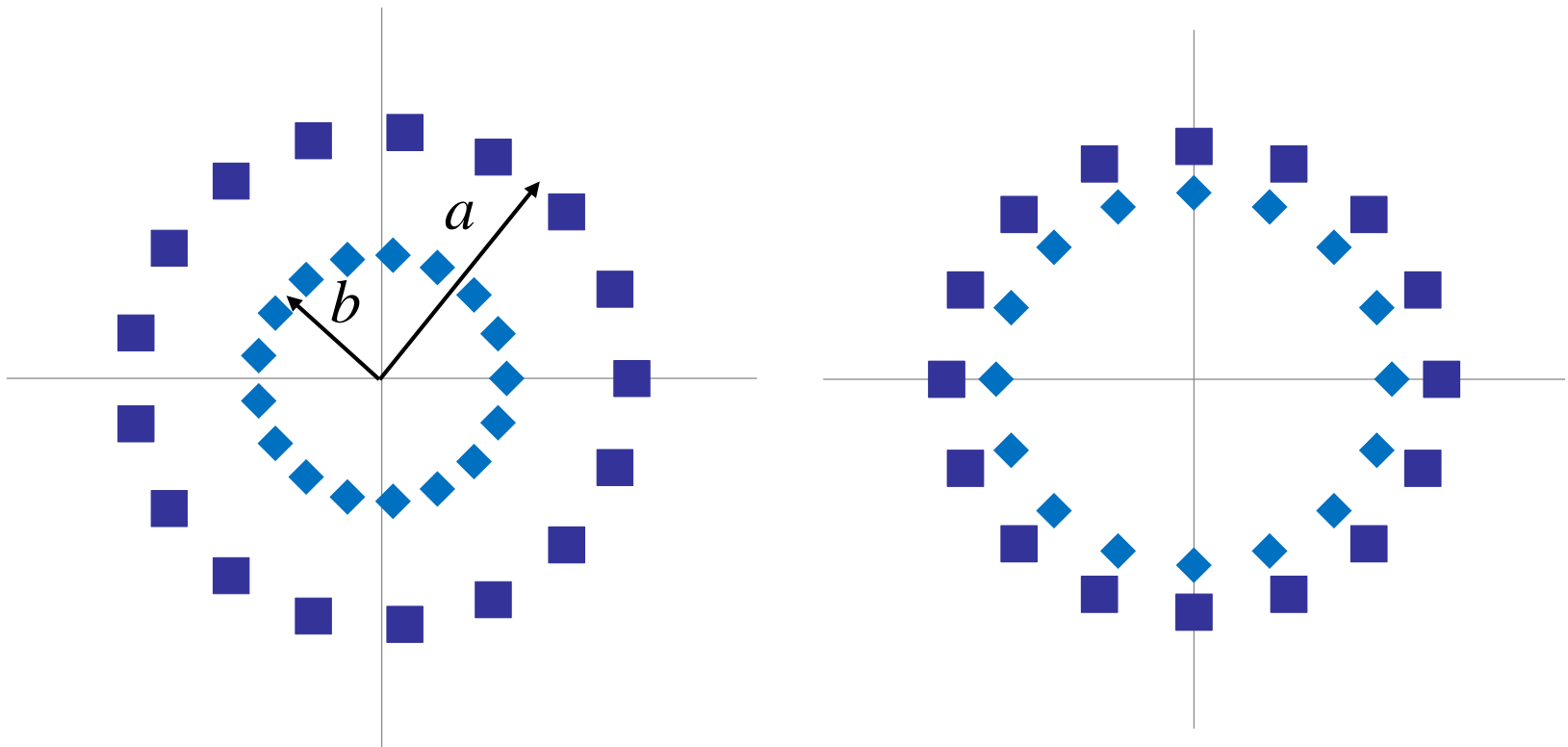
$$L_1 = 4$$

&lt;



$$L_2 = 2 + \sqrt{2}$$

# TSP for cities on concentric circles



$$r = \frac{b}{a}$$

## Complexity of TSP

Number of combinations to visit  $n$  cities is found to be

$$C = \frac{1}{2} (n - 1)!$$

The value of  $n!$  can be estimated by the Stirling approximation. For example, when  $n = 30$ ,  $C$  is estimated to be

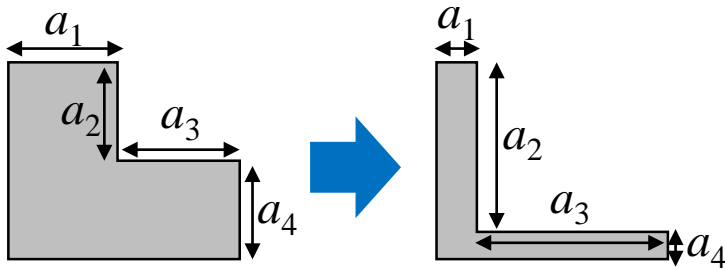
$$\begin{aligned} \log_{10} n! &\approx n(\log_{10} n - \log_{10} e) \\ &= n(\log_{10} n - 0.43) \approx 30 \end{aligned}$$

Core i7( $10^6$  Mips) executes an instruction for  $10^{-12}$  sec. Thus, roughly speaking,  $10^{18}$  sec =  **$10^9$  years (10億年)** lasts for  $10^{30}$  computations, that is, 30 city-problem.

# Shape Optimization

## Parameter Optimization

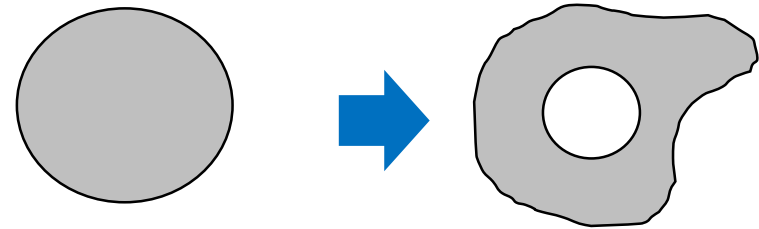
- Unknowns: design parameters



- Parameter design is necessary.
- Sound approach but little novelty

## Topology Optimization

- Shape is free deformed. Holes can be generated or annihilated.



- No parameter design
- Novel design might be obtained.

# Example of Topology Optimization

- The present method is applied to **magnetic shield** model shown below.
- The purpose of this optimization is to minimize the flux density in the target region and core volume in the design region.

## ■ Optimization Problem

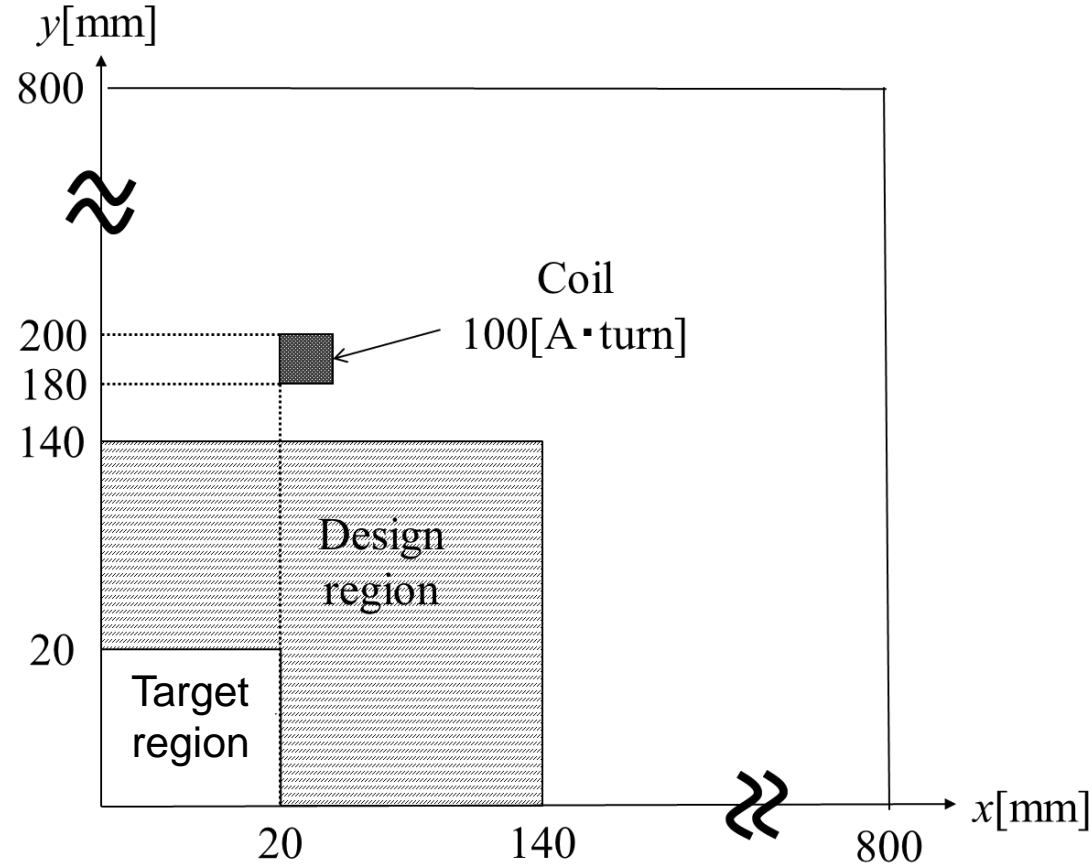
$$F(\phi) = W_M \frac{|B|_{average}}{10^{-5}} + \frac{S}{S_{design}} \rightarrow \text{Min.}$$

$W_M$ : weighting coefficient

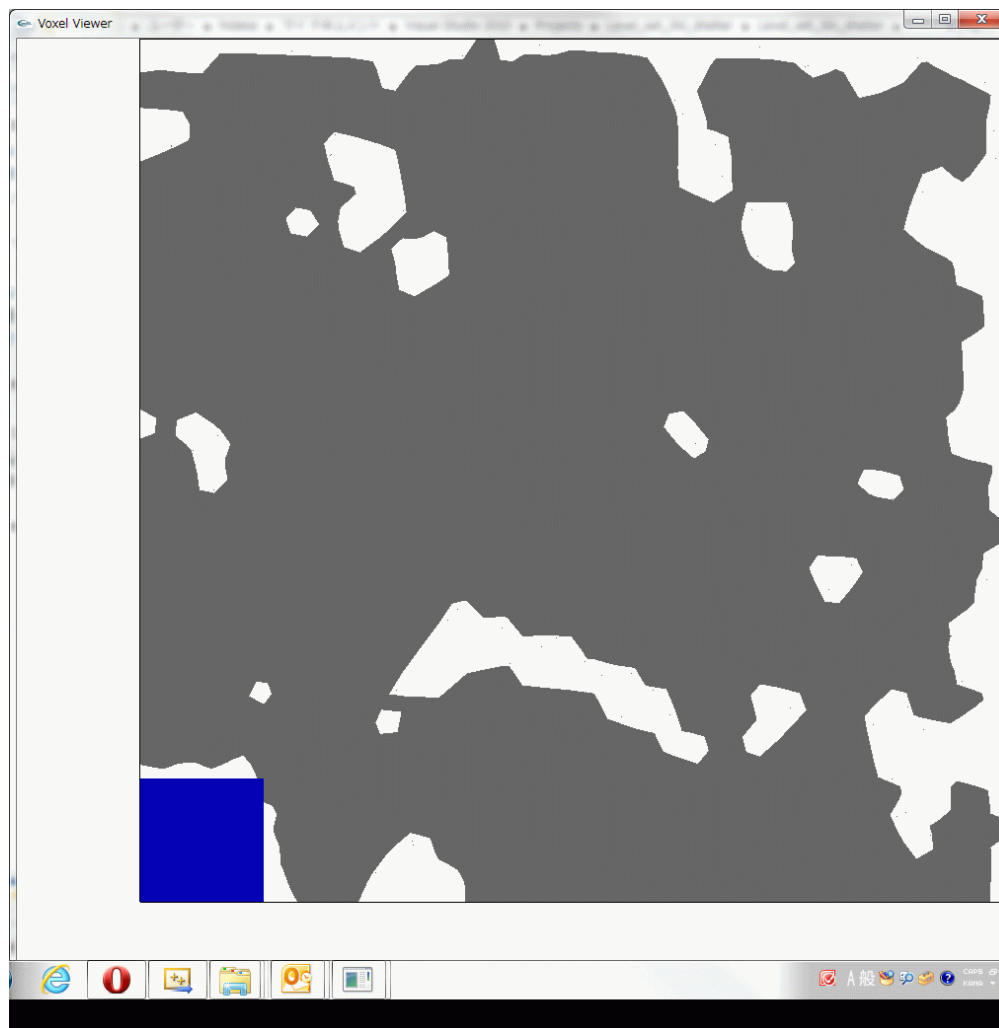
$S$ : core volume

$S_{design}$ : volume of the design region

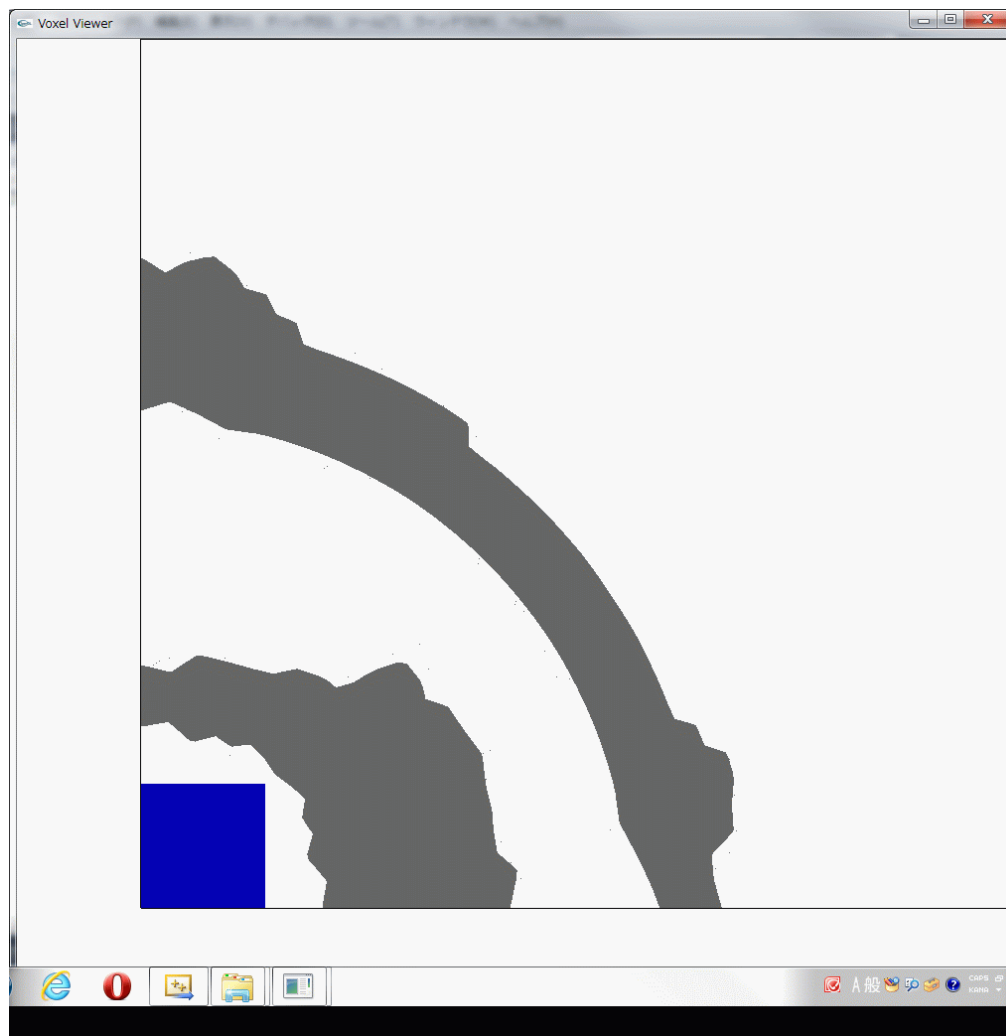
$B$ : flux density of in the target region



## Global search

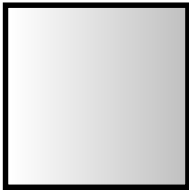
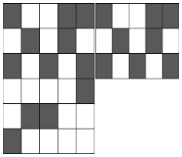
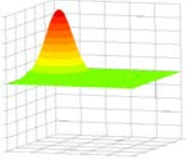


## Local search

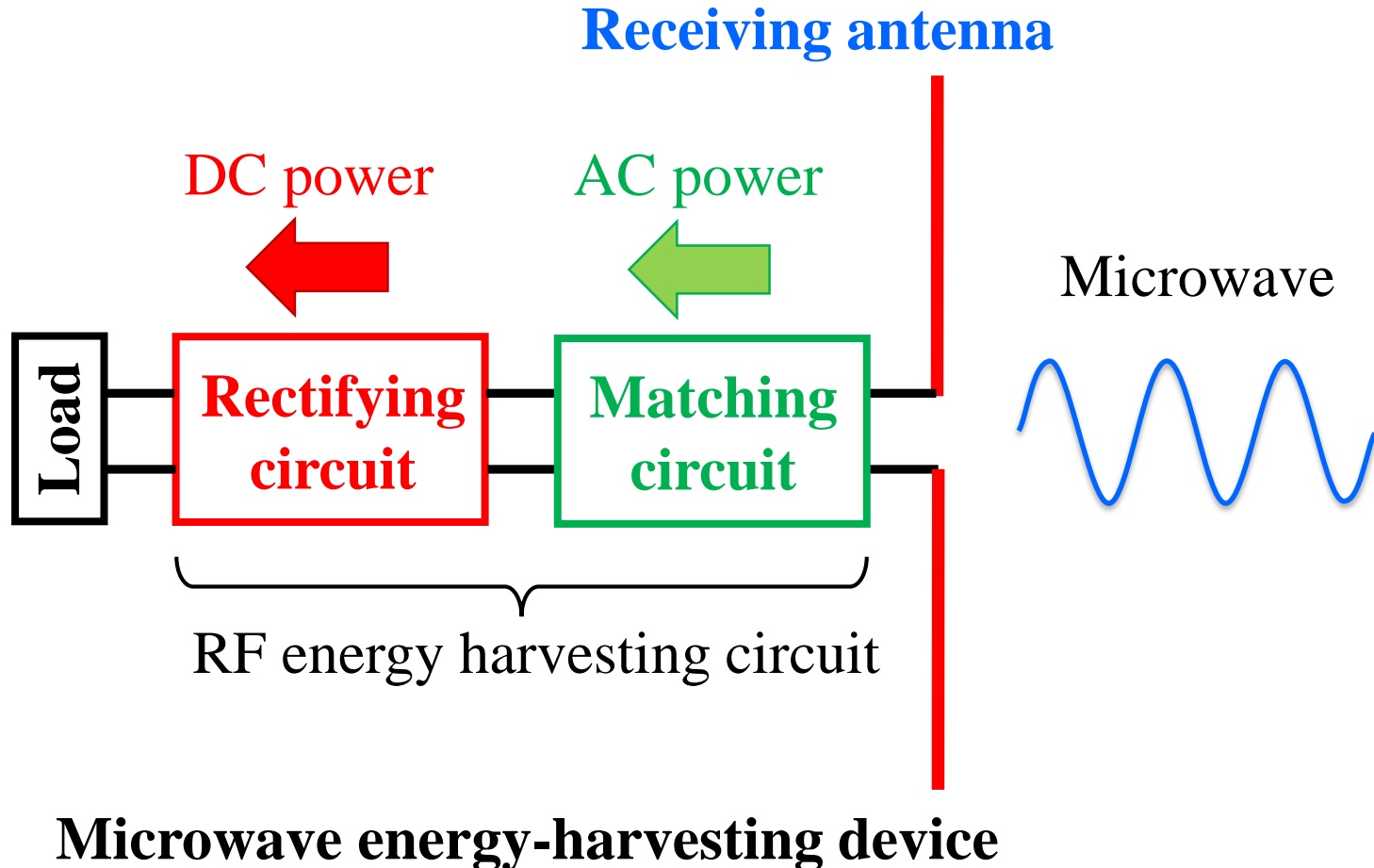


Y. Hidaka, T. Sato, H. Igarashi, "Topology Optimization Method Based on On-Off Method and Level Set Approach," IEEE Transactions on Magnetics, Volume:50, Issue:2, Article#7015204, 2014.

# Methods for Topology Optimization

| Methods   | Optimization                  | Features   |
|---|-------------------------------|--|
| Level set    | Sensitivity analysis          | 😊 Small comp. cost<br>😞 Derivative computation<br>😞 Local search   |
| Density    |                               |  |
| ON/OFF   | Stochastic algorithm, e.g. GA | 😞 Large computing cost<br>😊 No derivative comp.<br>😊 Global search |
| Basis function<br>$\psi(\mathbf{x}) = \sum_n w_n G_n(\mathbf{x})$  |                               |  |

- The microwave energy-harvesting device is composed of a receiving antenna and RF energy harvesting circuit.

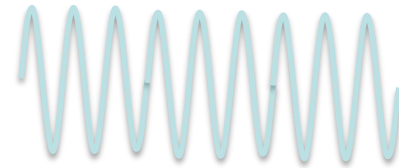


➤ We optimize the shape of receiving antenna and circuit parameters using optimization algorithm based on evolution technique.

➤ We consider harvesting energy from microwave transmitted by wireless router.

➤ The measured electric field intensity of 2.45GHz microwave is about 0.2V/m.

$$\underline{E \leq 0.2 \text{ [V/m] [1]}}$$



2.45GHz, 5.6GHz



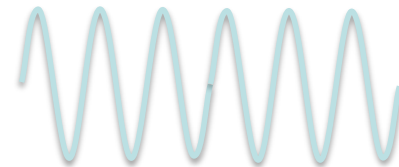
WiFi



100~800MHz



TV



700MHz~2.5GHz

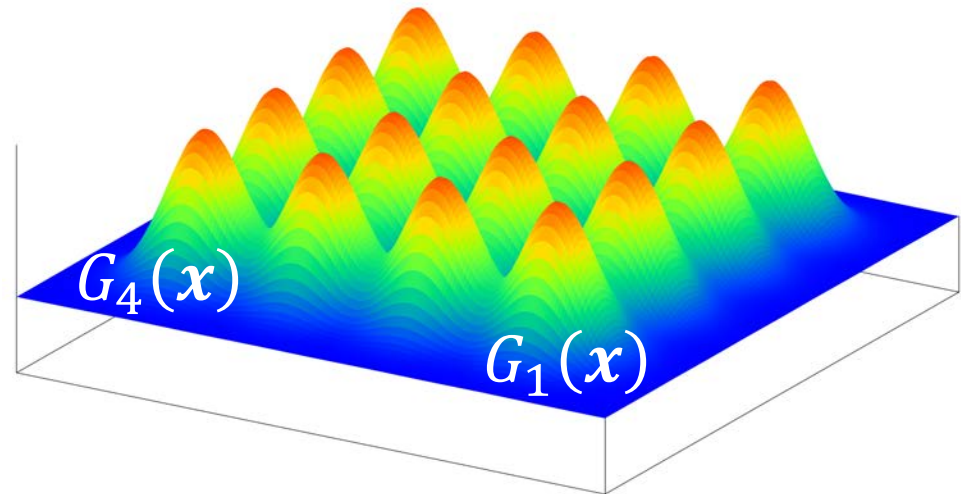
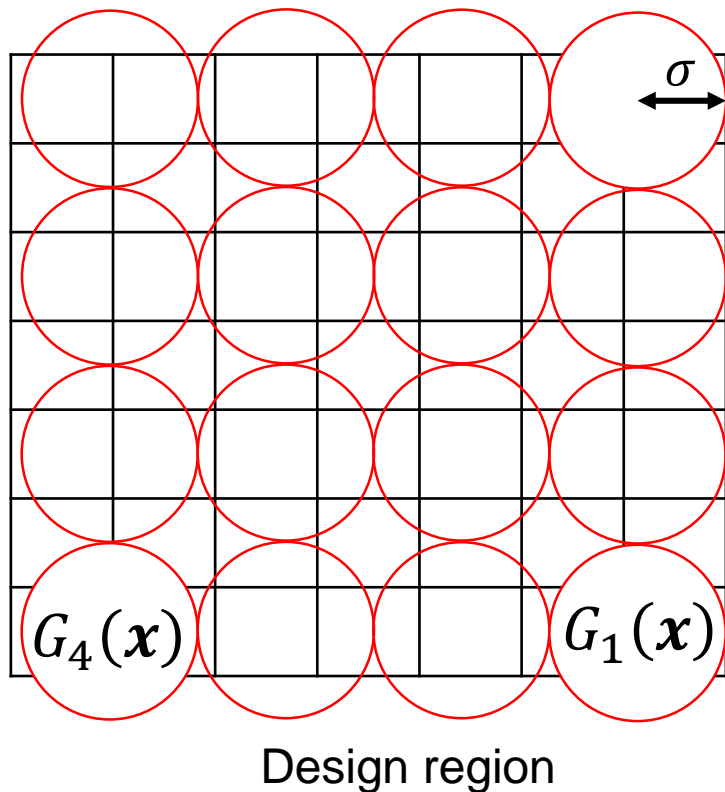


Smartphone

[1] Y. Kawahara, et al., "Power Harvesting from Microwave Oven Electromagnetic Leakage", *Proc. The 2013 ACM international Joint Conference on Pervasive and Ubiquitous Computing*, pp. 373-382, 2013.

# NGnet on/off method

Gaussian functions are uniformly deployed so that the design region is covered by the support of the Gaussians.



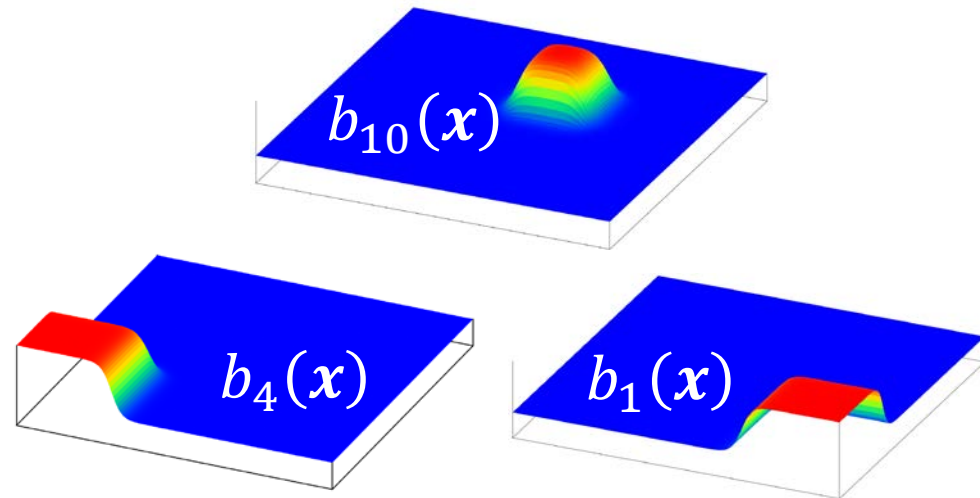
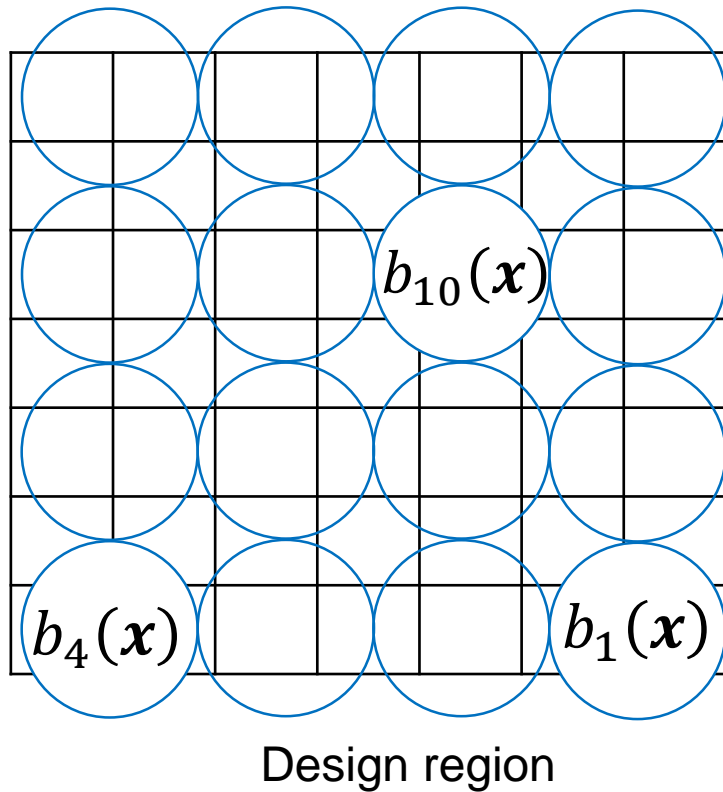
**Gaussian function**

$$G_i(\mathbf{x}) = \frac{1}{(2\pi\sigma)^{\frac{3}{2}}} \exp\left\{-\frac{1}{2\sigma^2} |\mathbf{x} - \mathbf{x}_i|^2\right\}$$

$\sigma$  : standard deviation

# NGnet on/off method

Gaussian functions in the design region are normalized.

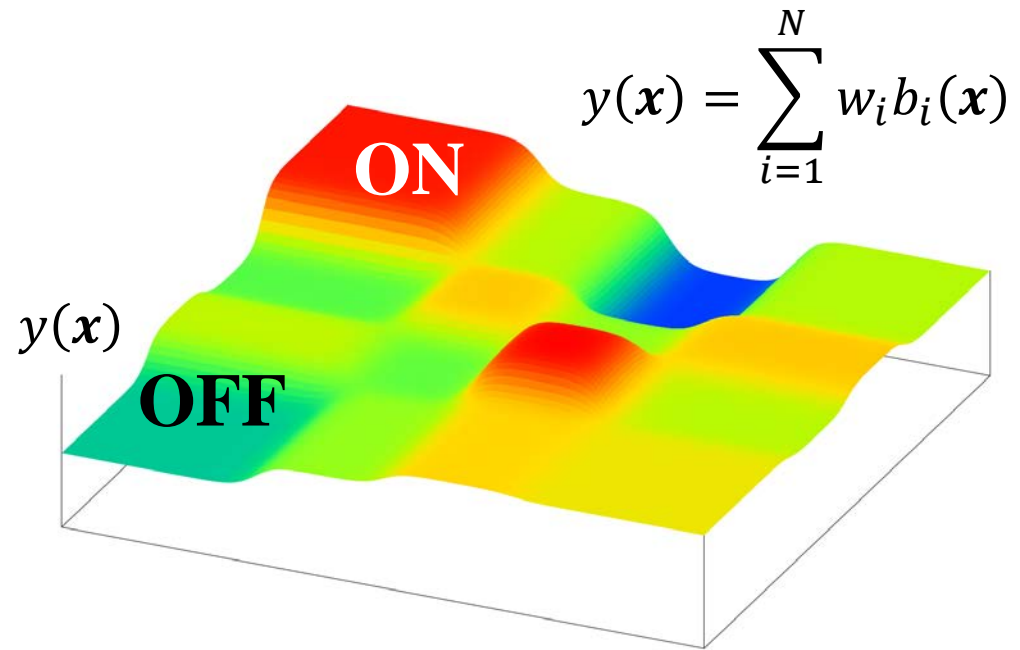
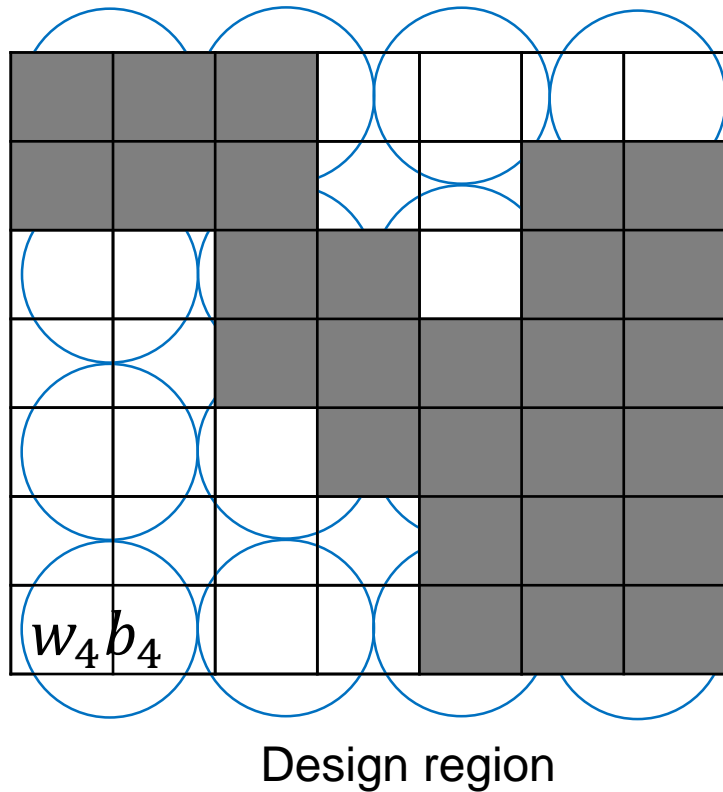


**Normalization**

$$b_i(\mathbf{x}) = G_i(\mathbf{x}) / \sum_{j=1}^N G_j(\mathbf{x})$$

# NGnet on/off method

To determine the material attribute in the design region, we use the output of the shape function  $y(\mathbf{x})$ .



**Material attribute**

$$M_e = \begin{cases} \text{ferrite (ON)} & y(\mathbf{x}) \geq 0 \\ \text{air (OFF)} & y(\mathbf{x}) < 0 \end{cases}$$

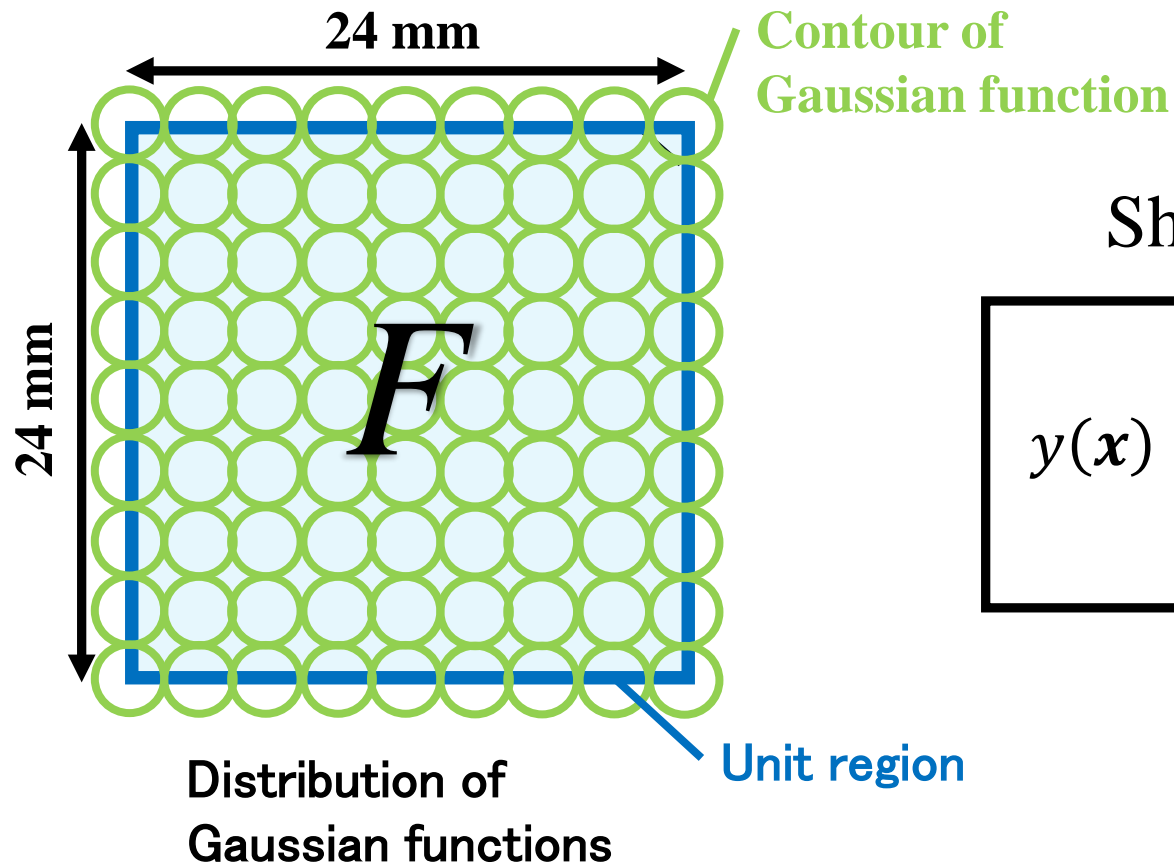


:air



:ferrite

The Gaussian functions are uniformly deployed in the unit region whose direction is represented by “ $F$ ”.



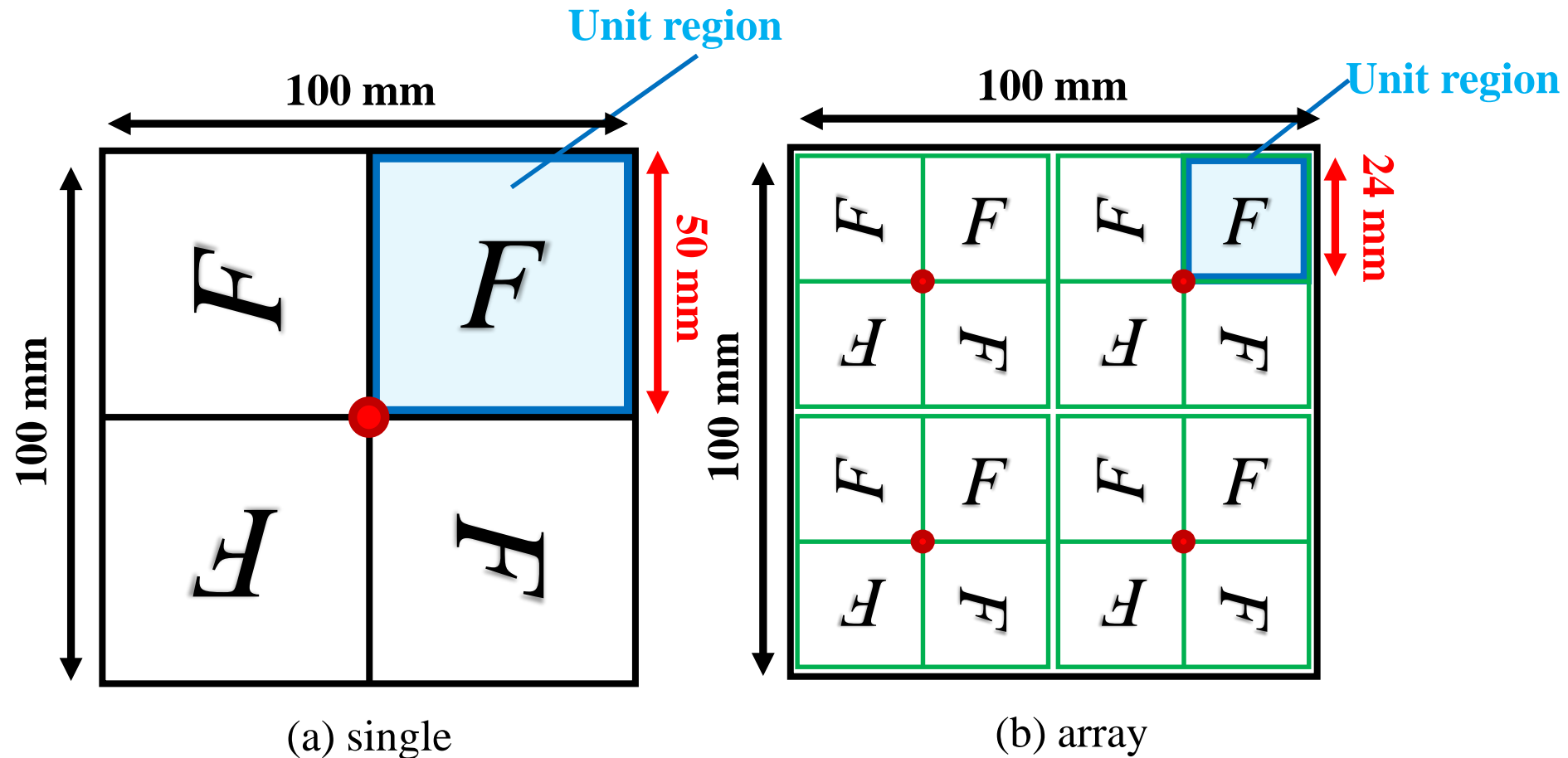
Shape function

$$y(\mathbf{x}) = \sum_{i=1}^N w_i b_i(\mathbf{x})$$

$N=81$

The single antenna consists of four unit regions with  $C_4$  symmetry.

The array antenna consists of four  $4 \times 4$  unit regions with  $C_4$  symmetry.



# Optimization Problem

The actual gain is maximized in the frequency period (1.5GHz, 3.5GHz).

$$\langle G_{actual} \rangle = \frac{\int_{f_0}^{f_1} G_{actual}(f) df}{f_1 - f_0} \rightarrow \max$$

$$G_{actual}(f) = \frac{1}{4} \sum_{k=1}^4 G_{iso}(f) \left( 1 - \left| \frac{Z_a^k(f) - Z_c}{Z_a^k(f) + Z_c} \right|^2 \right)$$

impedance matching

$G_{actual}$  : actual gain

$G_{iso}$  : absolute gain

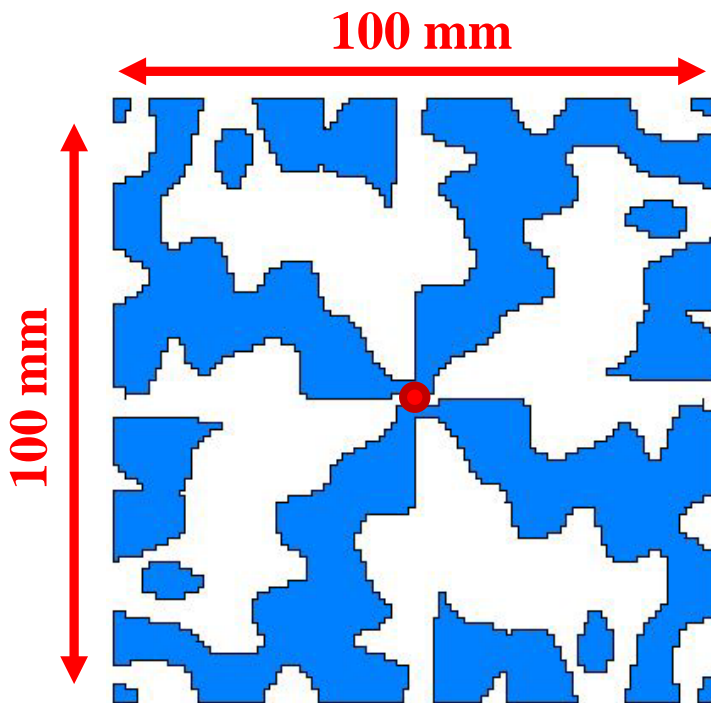
$Z_a$  : input impedance of antenna

$Z_c = 50 \Omega$  : input impedance of circuit

$f_0 = 1.5 \text{ GHz}$

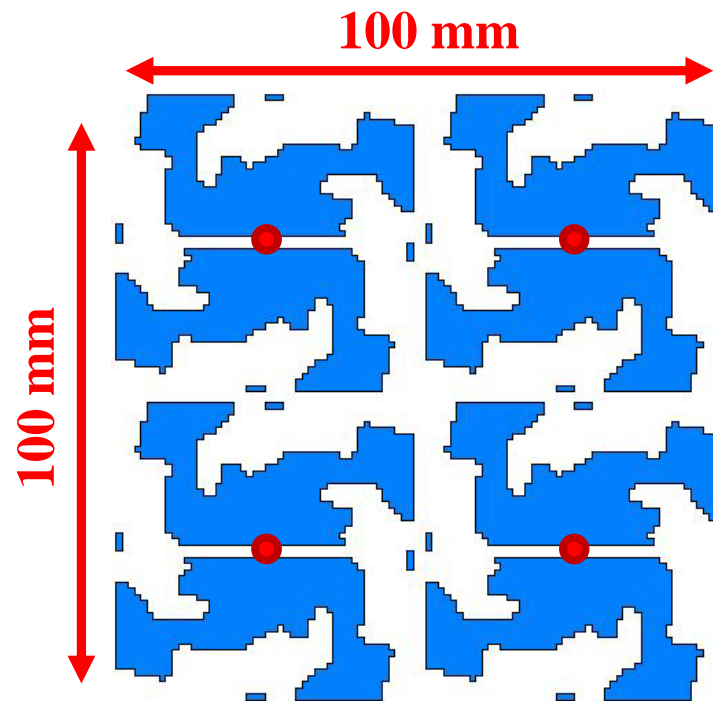
$f_1 = 3.5 \text{ GHz}$

# Optimal Shapes



(a) single

$$\langle G_{actual} \rangle = 5.6 \text{ dBi}$$

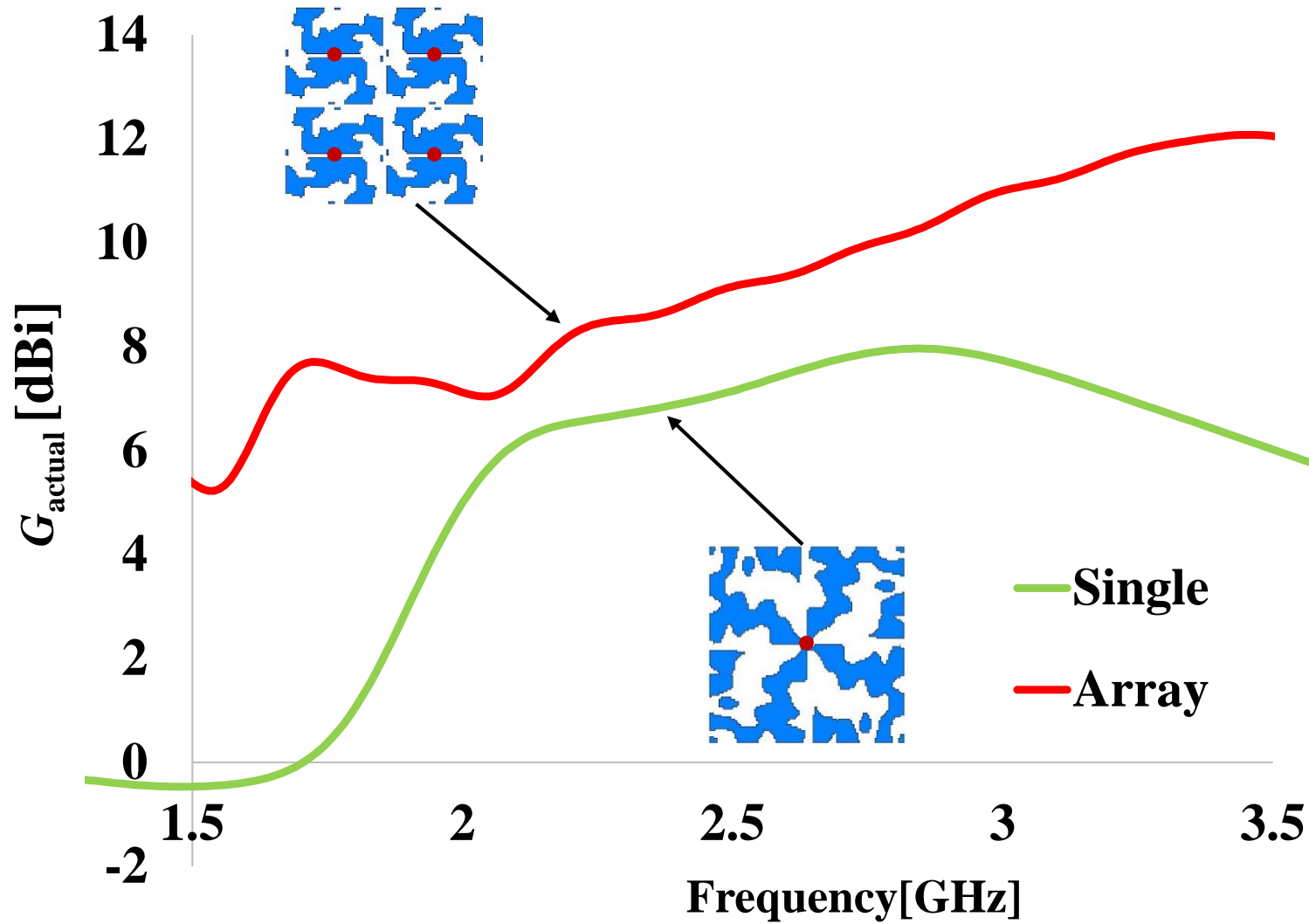


(b) array

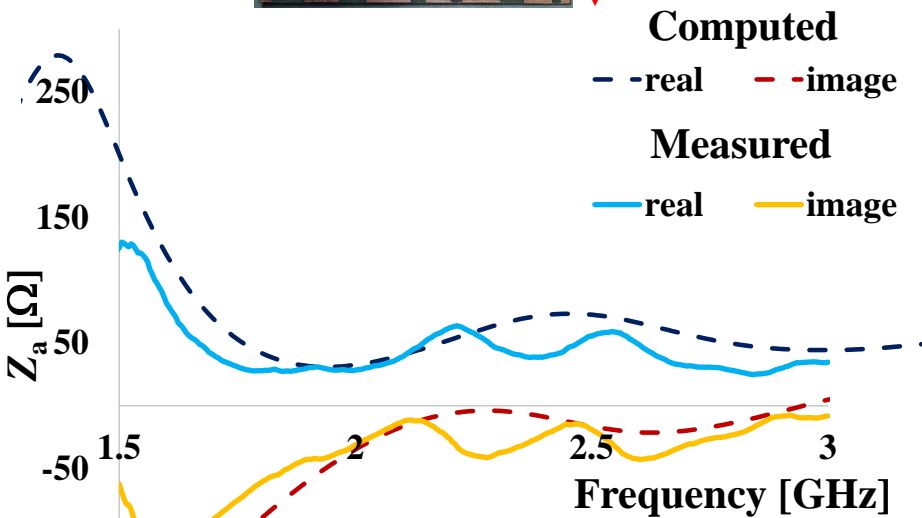
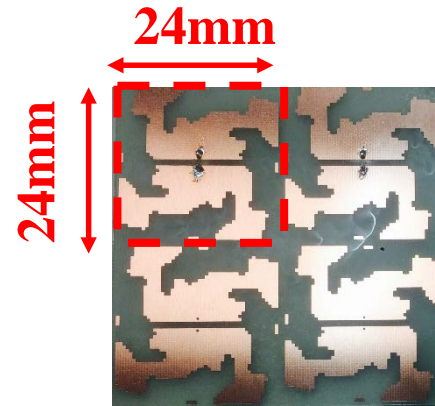
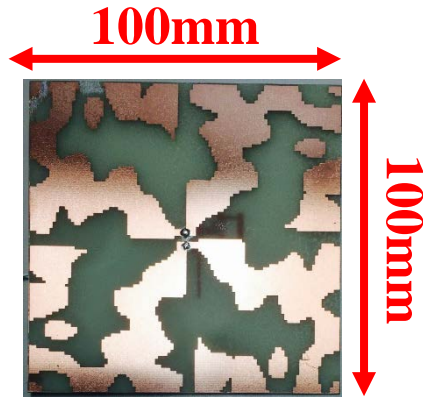
$$\langle G_{actual} \rangle = 9.2 \text{ dBi}$$

T. Mori, H. Igarashi, Topology optimization of wideband array antenna for microwave energy harvester, International Journal of Applied Electromagnetics and Mechanics, vol. 52, no. 1-2, pp. 631-639, 2016.

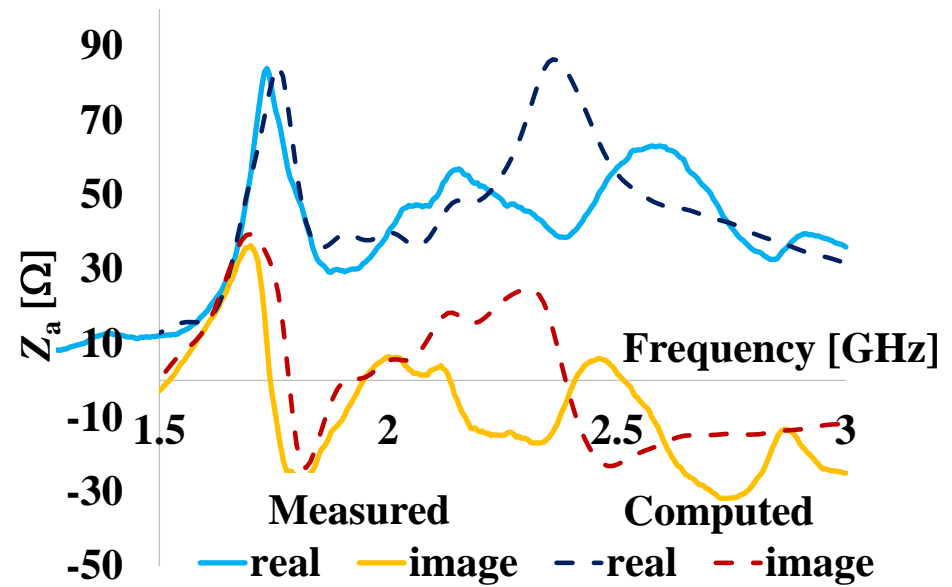
# Optimization result



# Computed and measured input impedance

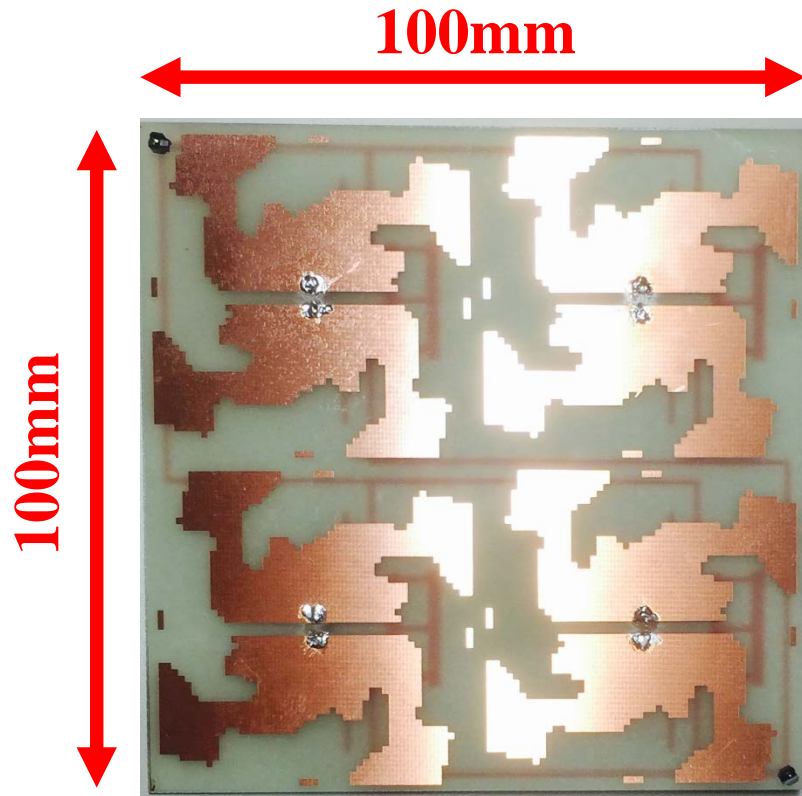


(a) single

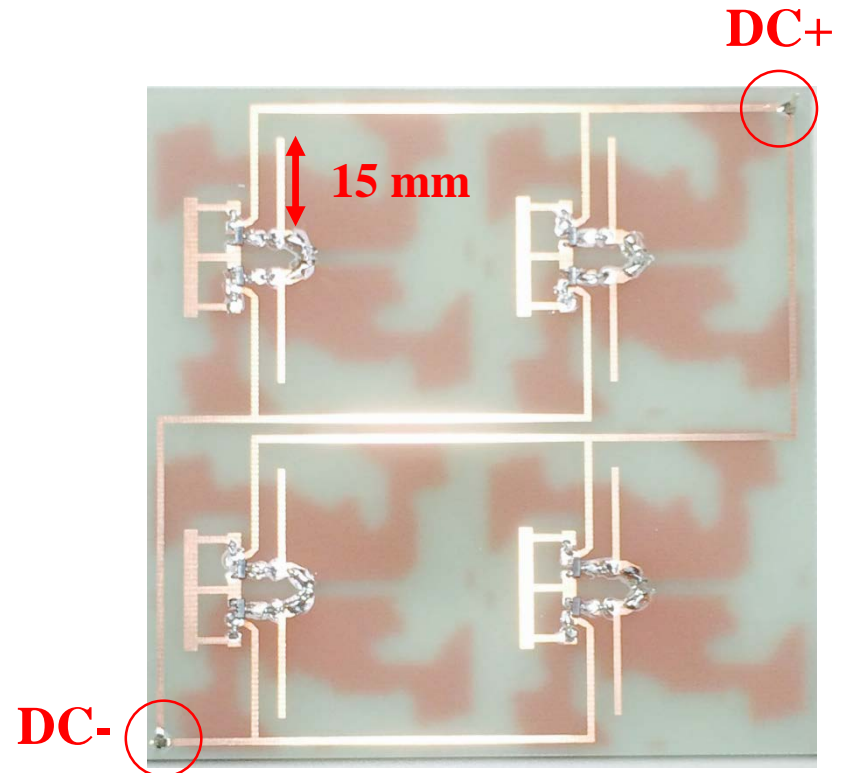


(b) array

# Realization of optimized antenna



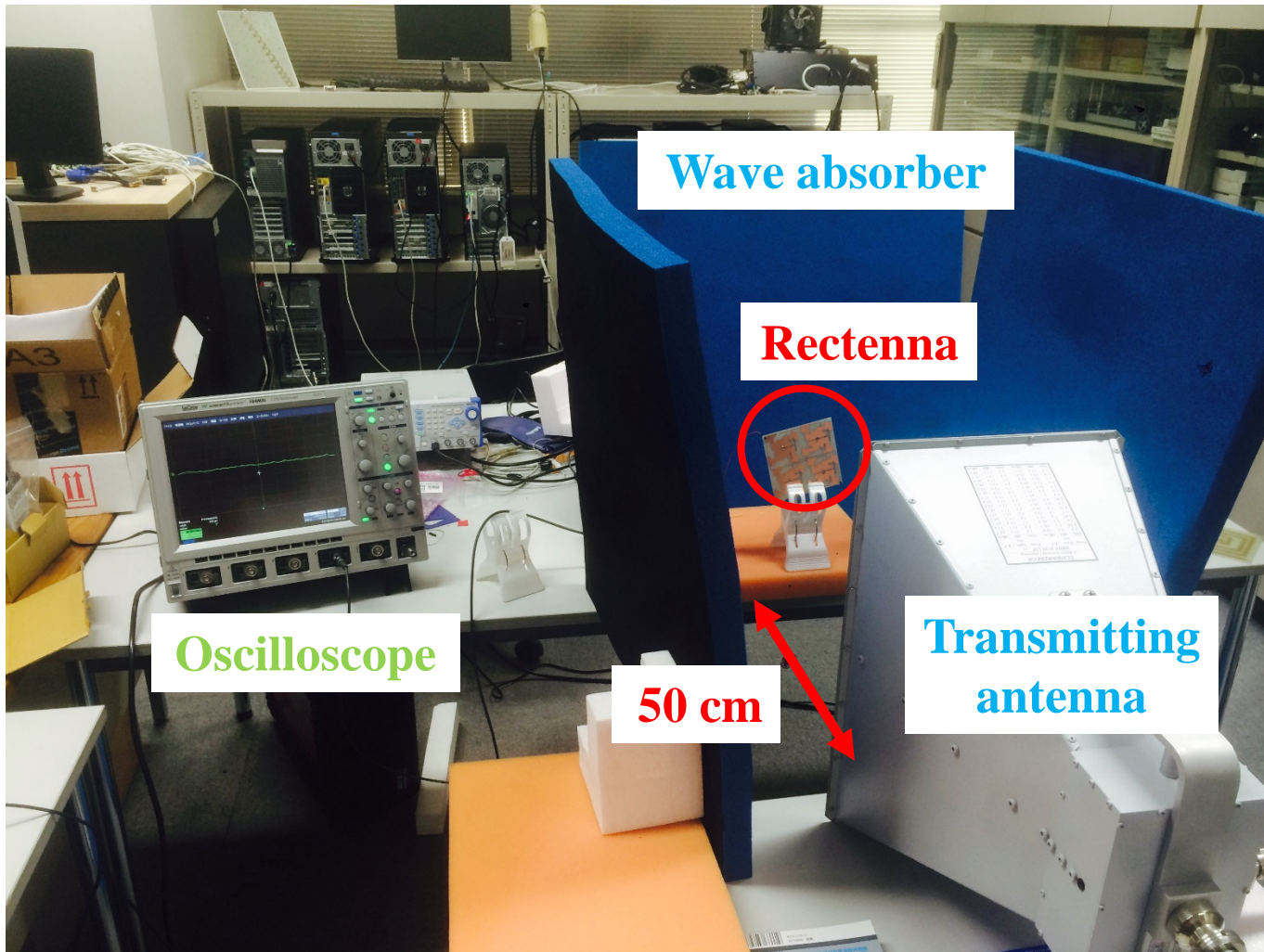
(a) front face

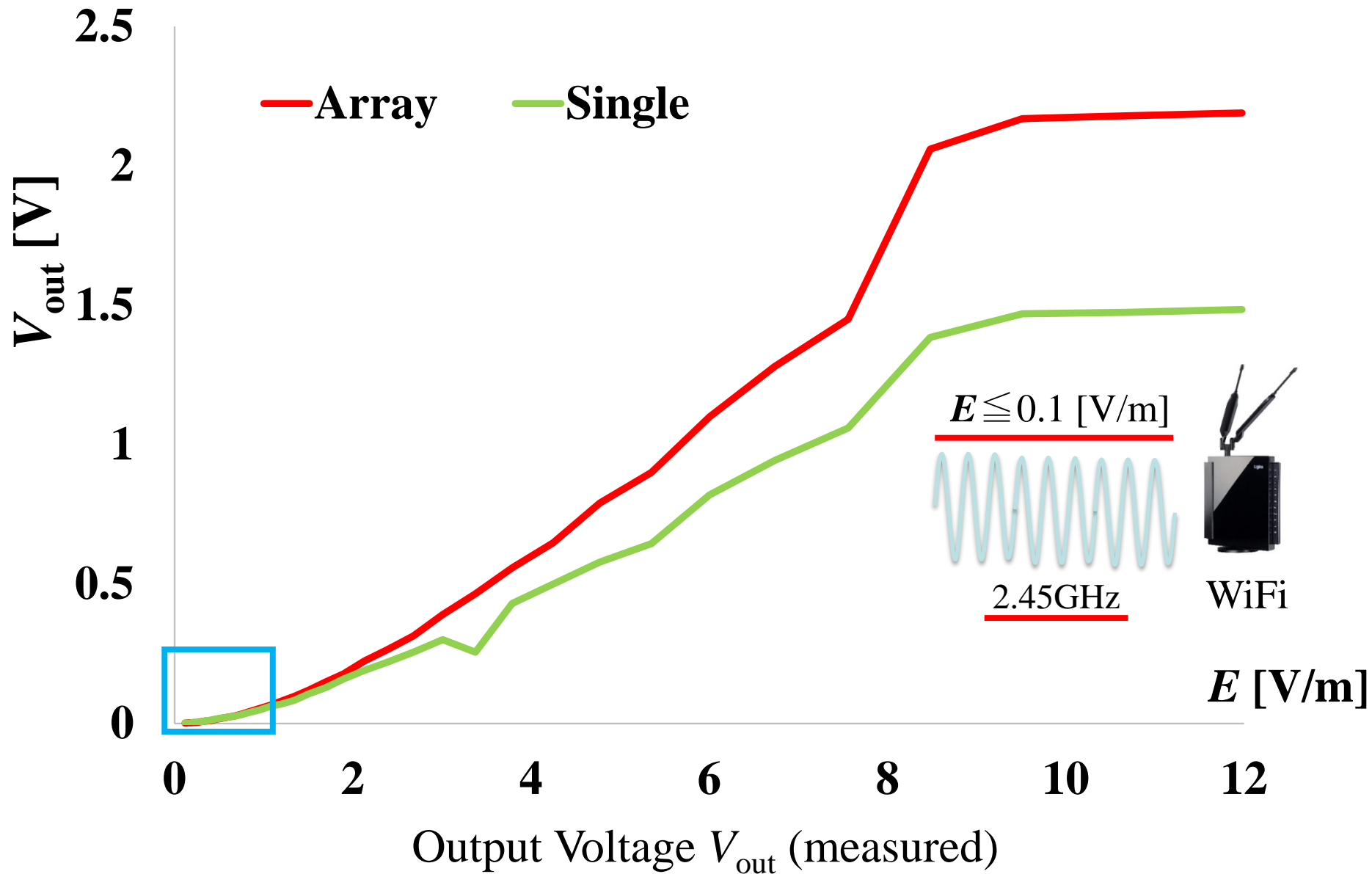


(b) back face with circuit

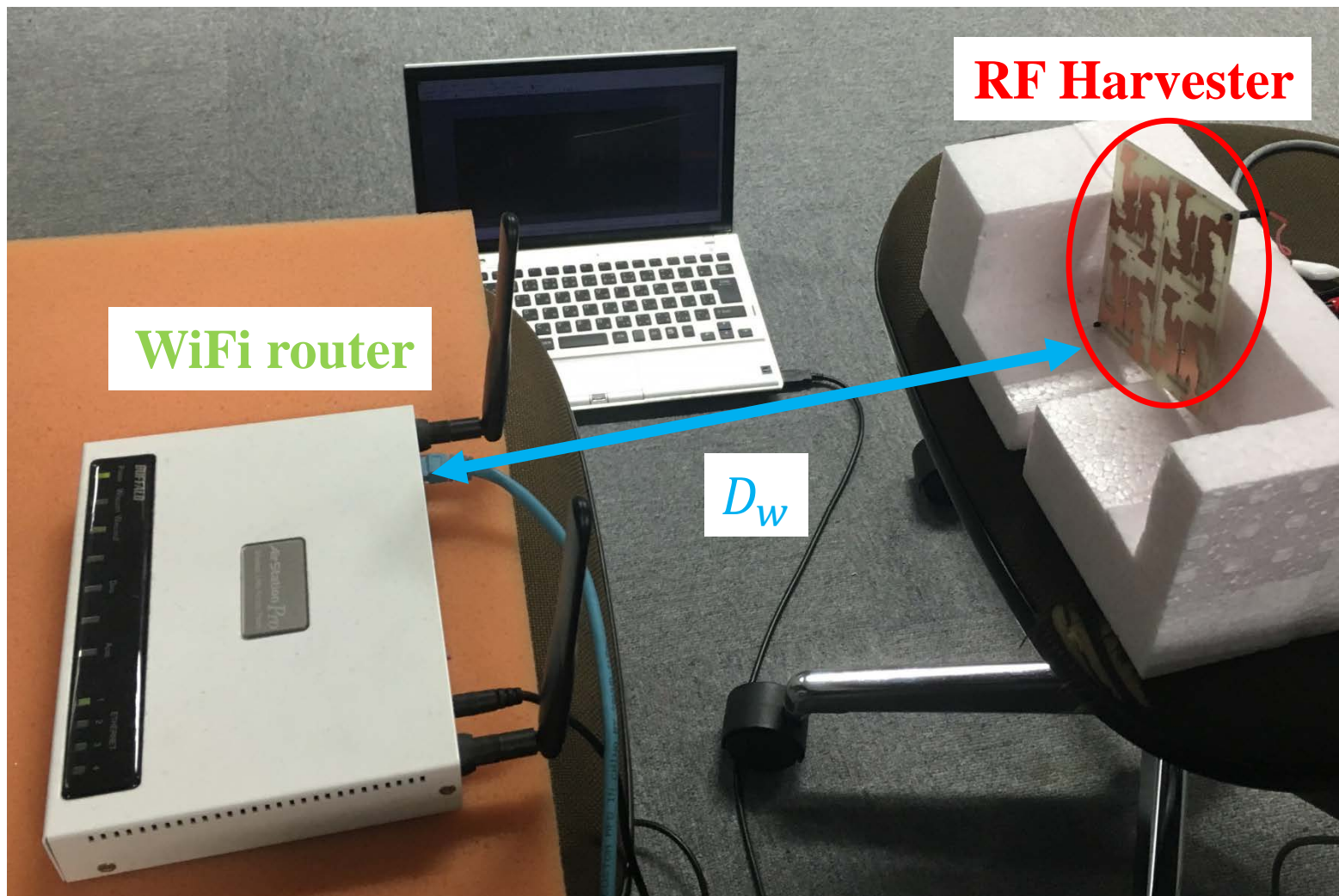
Manufactured Array Antenna

# Measurement of output voltage

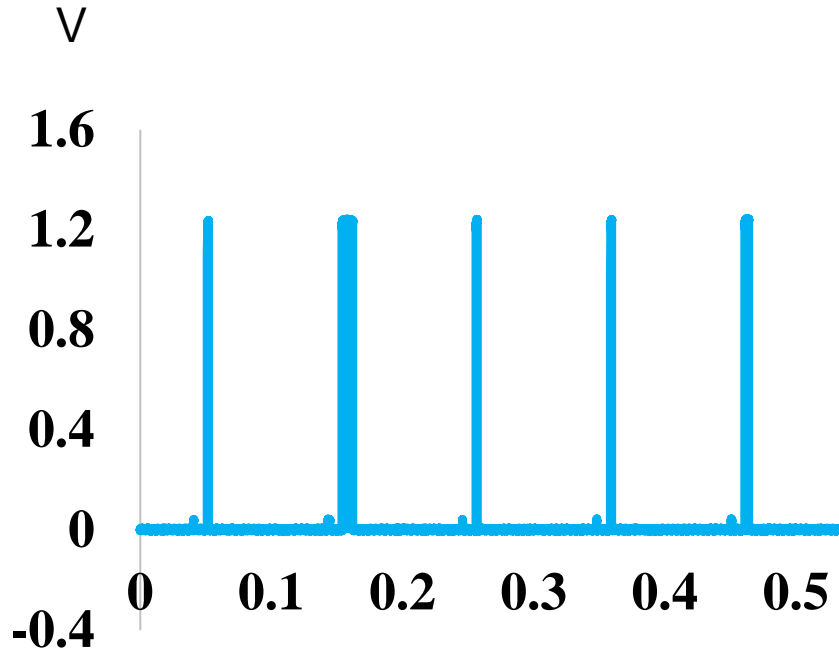




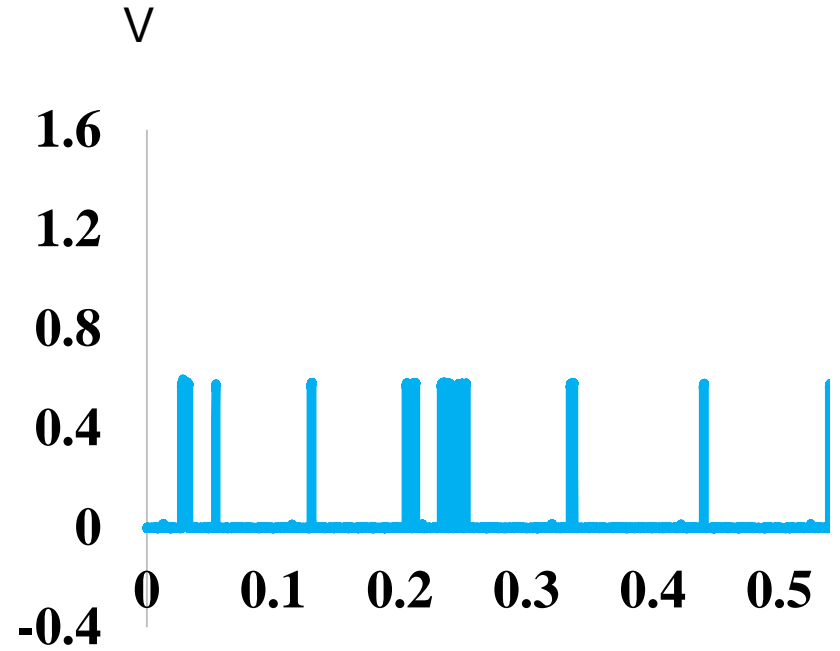
## Operation test: RF harvester located near WiFi router



# Voltage generated by harvester



$D_W = 15\text{cm}$



$D_W = 30\text{cm}$

## From Hybrid Vehicle (HV) to Zero Emission Vehicle (ZEV)

For manufacturers with annual sales greater than 60,000 vehicles, at least 14% of the vehicles they produce and deliver for sale in California must meet ZEV requirements for 2015 through 2017.

# Optimization of Wireless Power Transfer

- Wireless power transfer (WPT) for EVs is expected to expand rapidly.

WPT system for EVs

Y. Otomo, Y. Gong, H. Igarashi, 3-D Topology Optimization of Magnetic Cores for Wireless Power Transfer with Double-Sided Shielding Coils, presented at OIPE2018, submitted to Int. J. AEM.



# Optimization problem

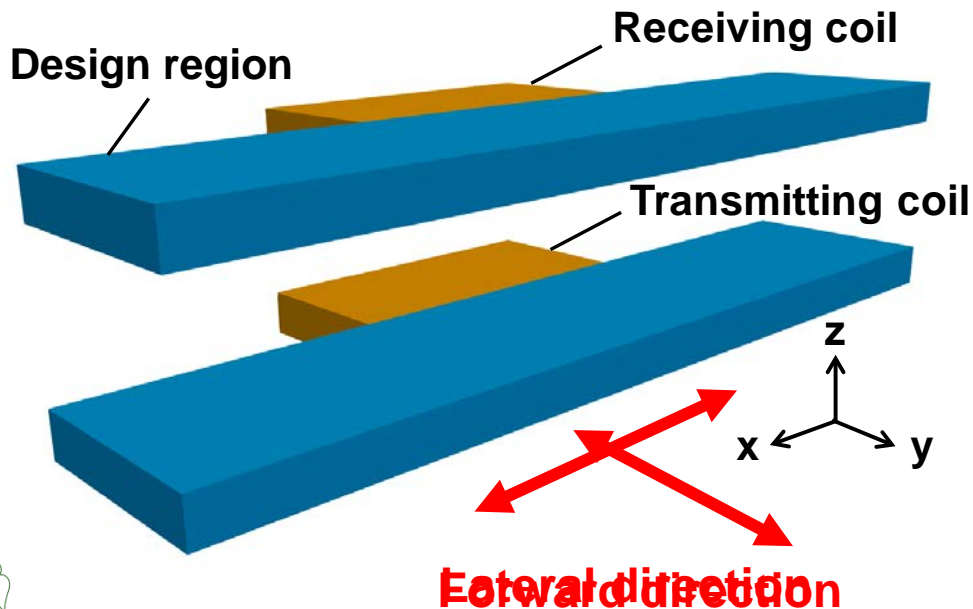
## Optimization problem

$$\max_{\mathbf{w}} F(\mathbf{w}), \quad F(\mathbf{w}) = \frac{1}{N_p} \sum_{i=1}^{N_p} k_i(\mathbf{w}), \quad \text{sub. to } \Omega_M \leq \frac{\Omega_D}{2}$$

$k_i(\mathbf{w})$  : coupling coefficient of the  $i$ -th misalignment

$\Omega_M$  : total volume of the magnetic core

$\Omega_D$  : volume of the design region



## Three different misalignments

0 mm

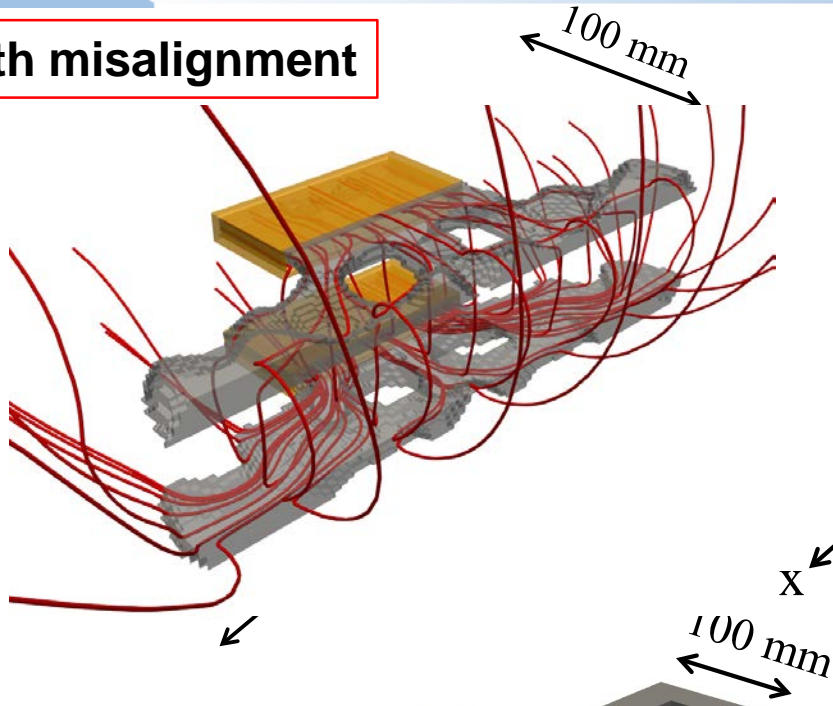
150 mm



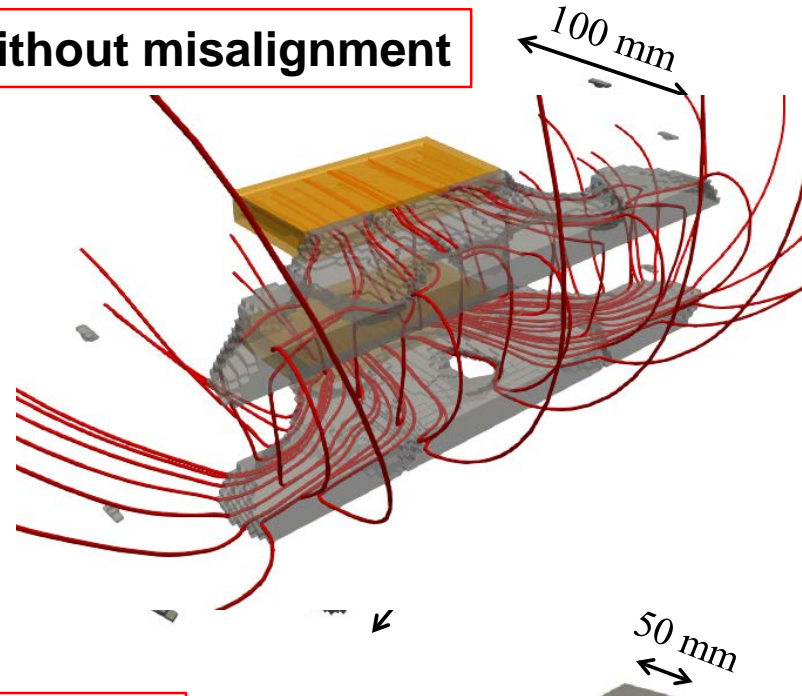
300 mm

# Optimized and conventional core shapes

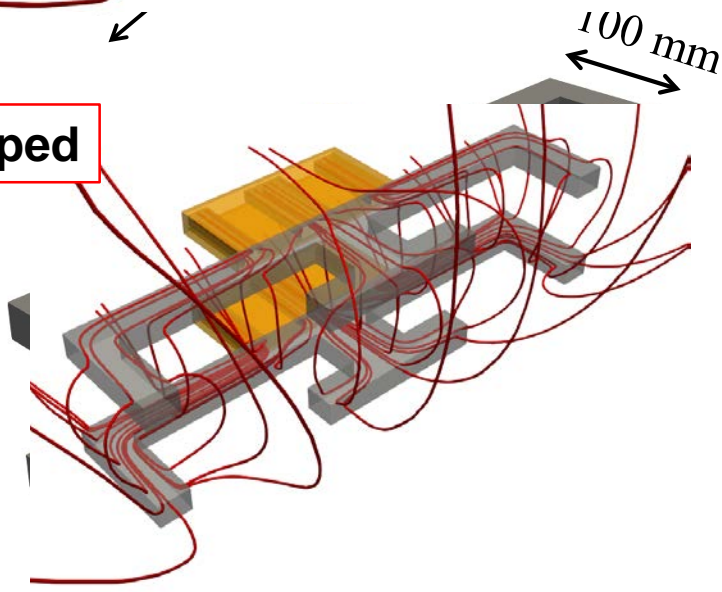
**With misalignment**



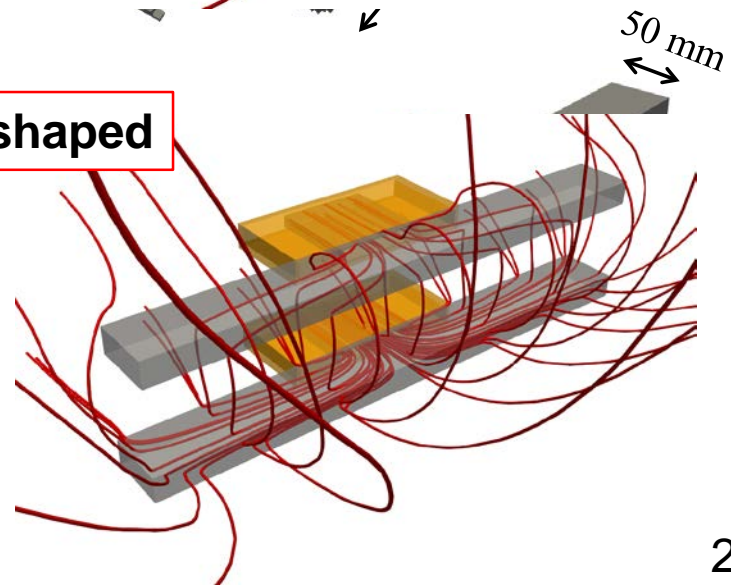
**Without misalignment**



**Bar shaped**

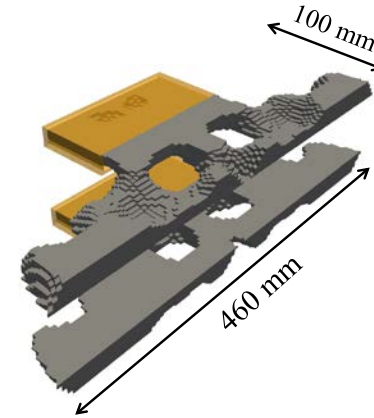
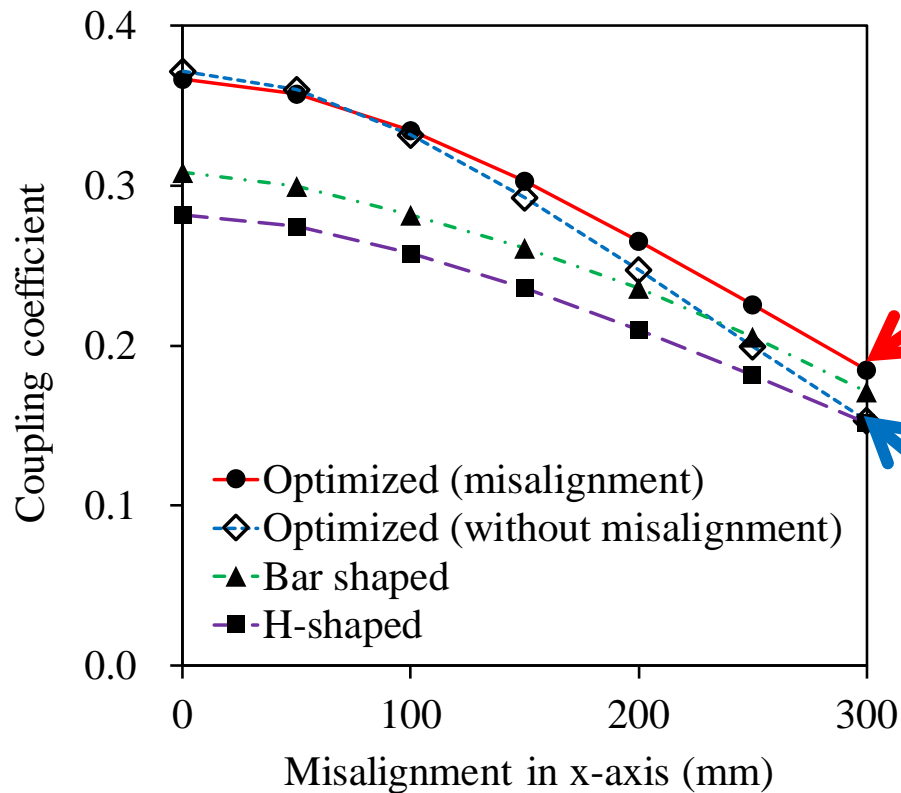


**H-shaped**

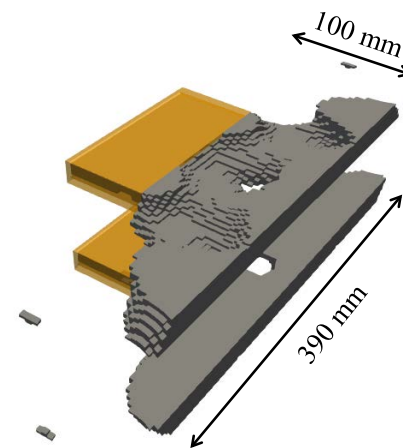


# Coupling coefficient of each WPT core

- We can see that the optimized WPT cores have the good tolerance in the forward misalignment and air gap.

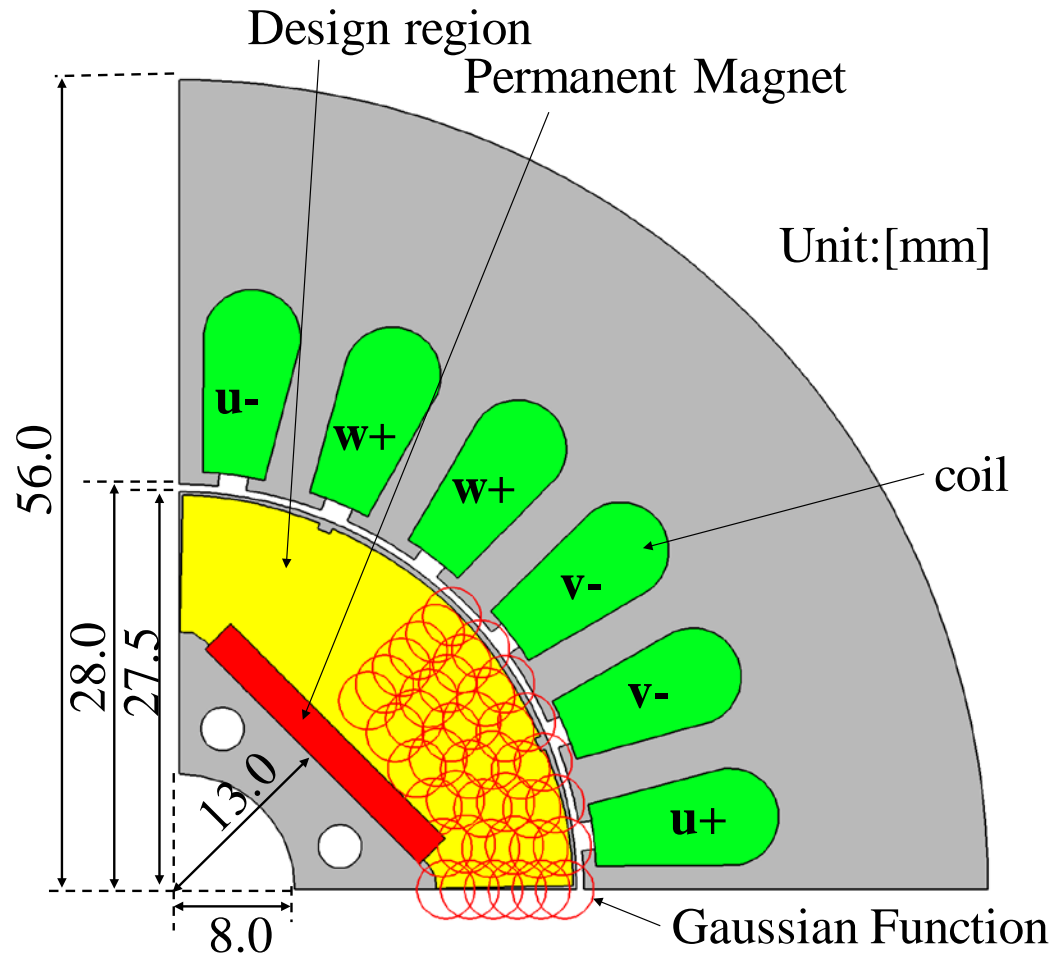


**(a) with misalignment**

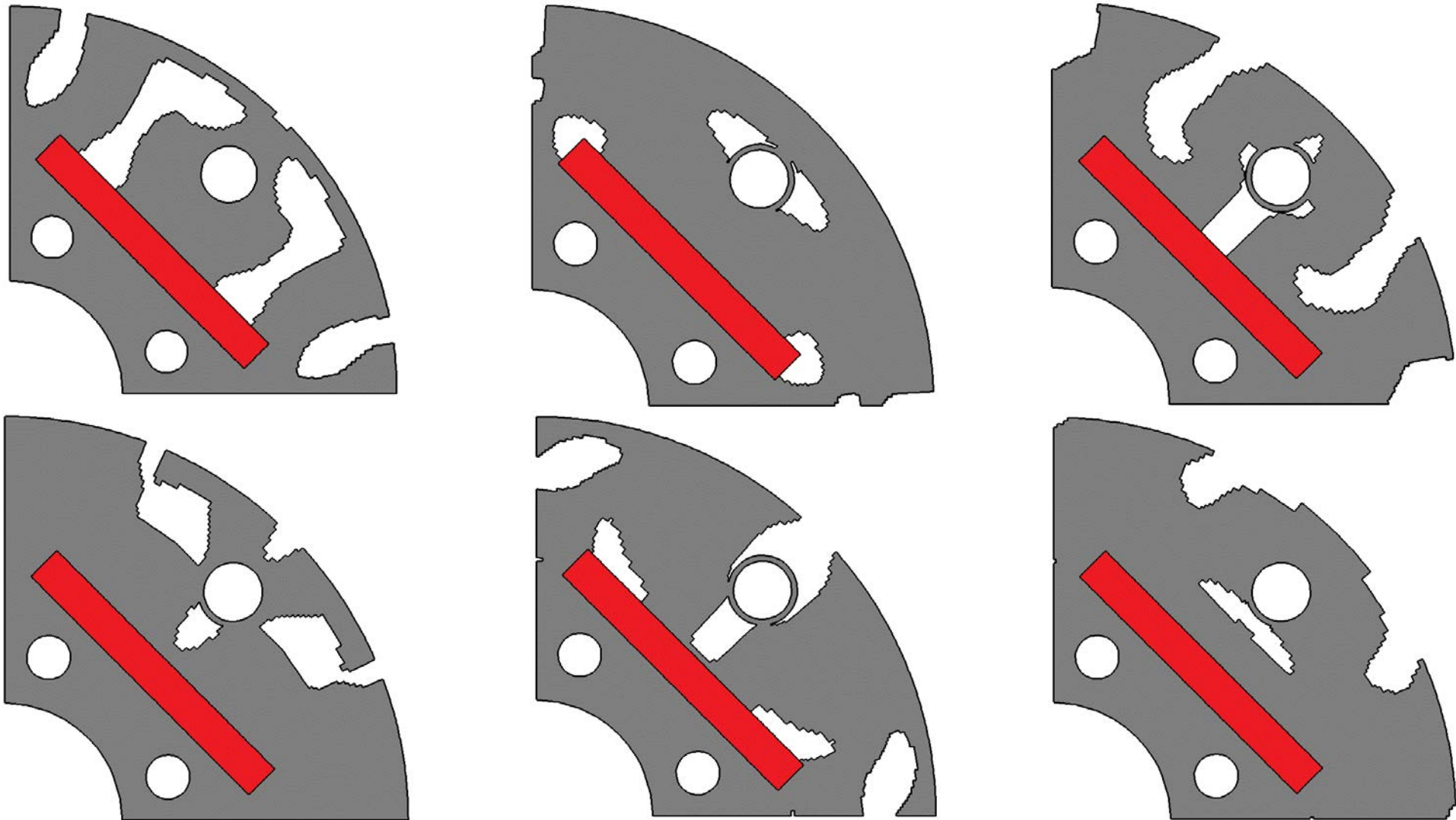


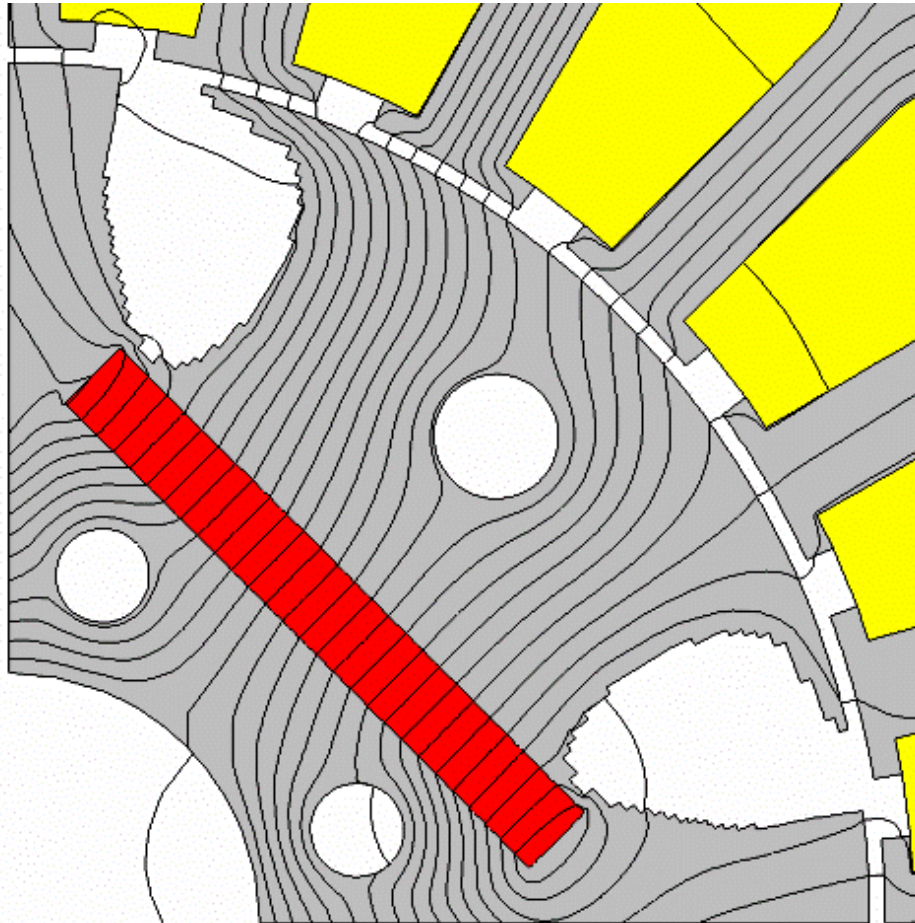
**(b) without misalignment**

# Optimization of Interior Permanent Magnet (IPM) Motor



# Initial individuals generated in the GA process





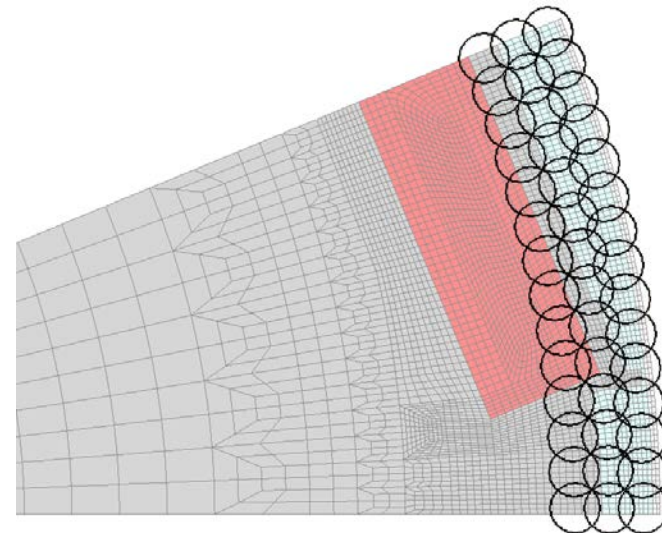
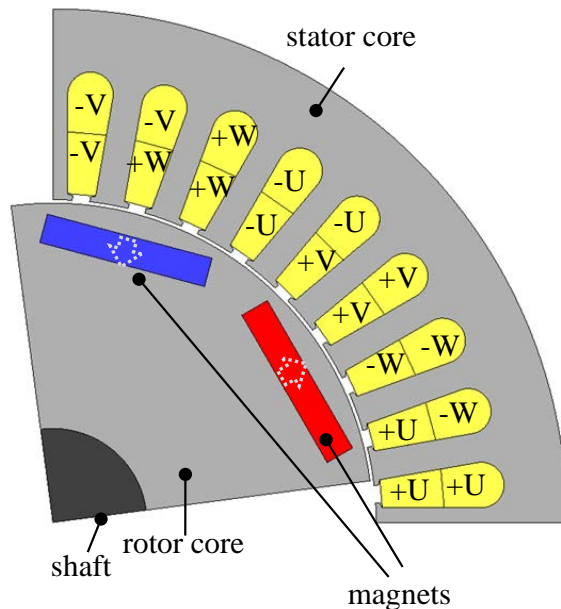
# Optimization of Realistic IPM Motor

Maximization of torque and minimization of ripple

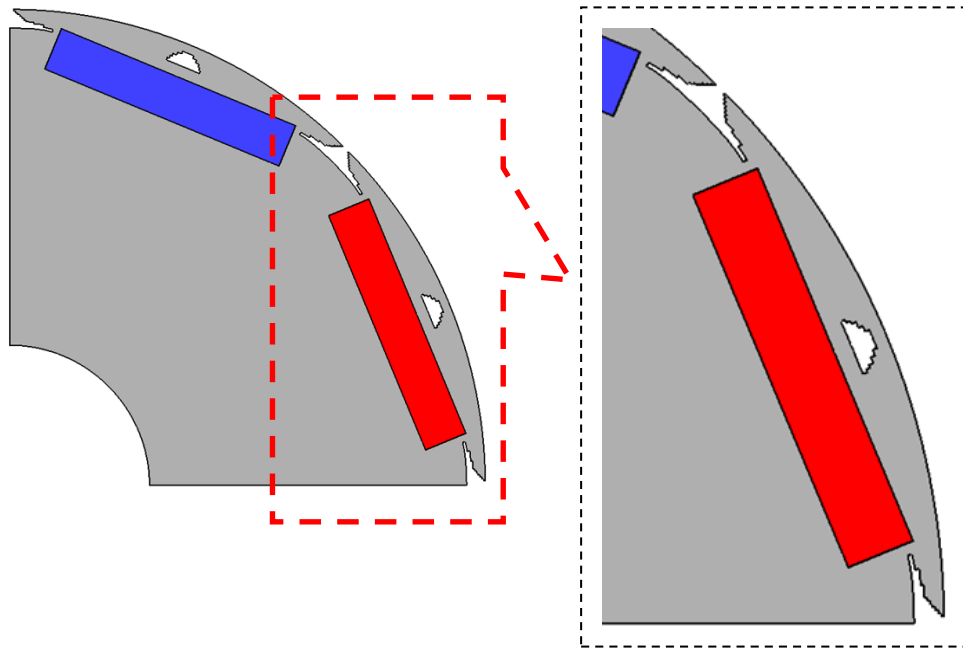
$$F = -T_{ave}/T_0 + 0.5T_{rp}/T_1 \rightarrow \text{minimize,}$$

$T_{ave}$ : average torque,  $T_{rp}$ : torque ripple

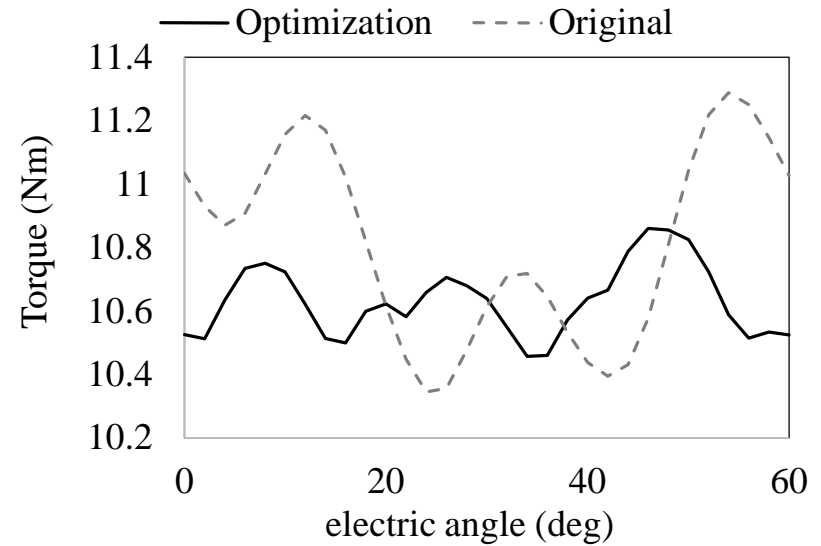
$T_0=10.8\text{Nm}$ ,  $T_1=8.5\%$ : normalization constants



# Optimization result

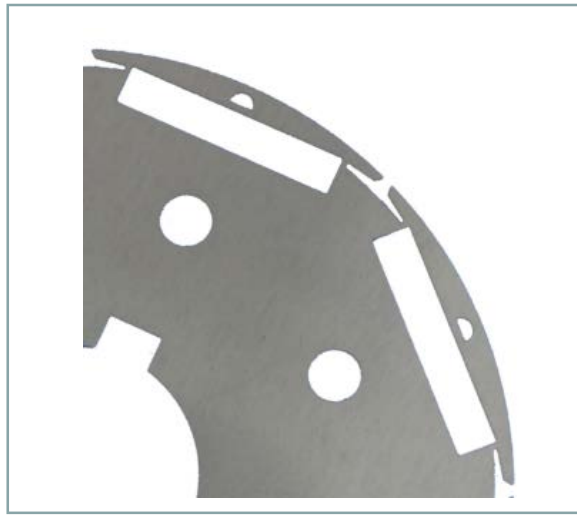


$T_{ave}=0.96T_0, T_{rp}=0.25T_1$

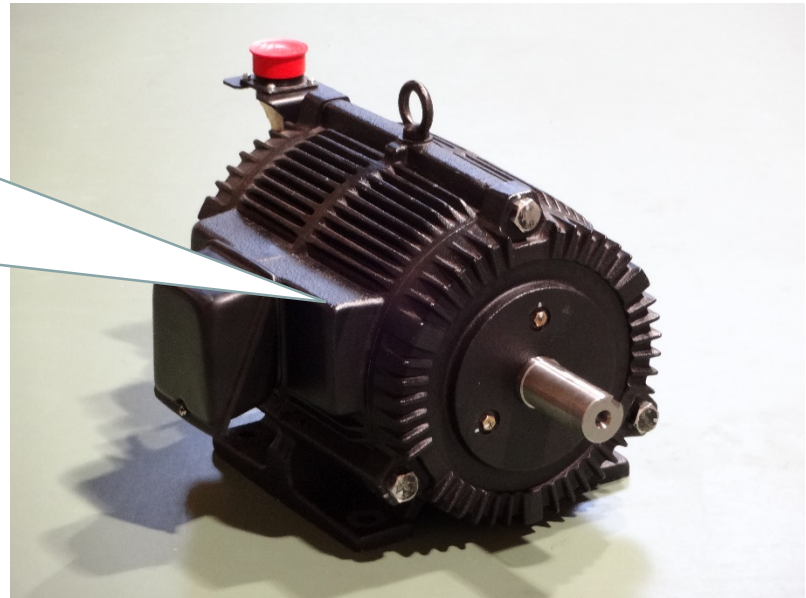


Torque ripple is greatly reduced by the optimization.

## Realization of Optimized IPM Motor



Manufactured rotor

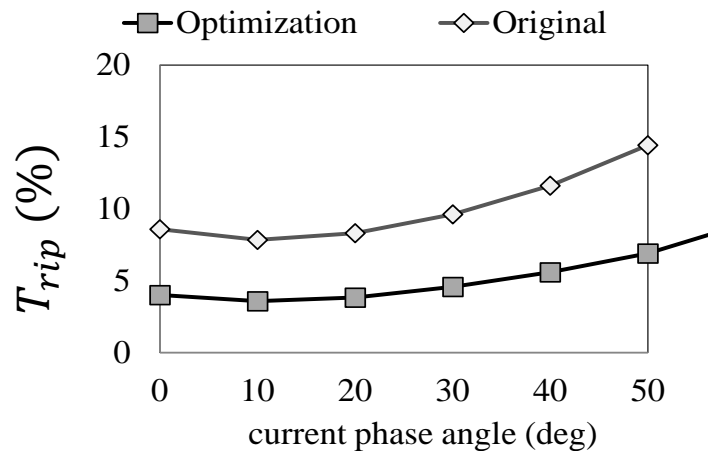


# Experimental results

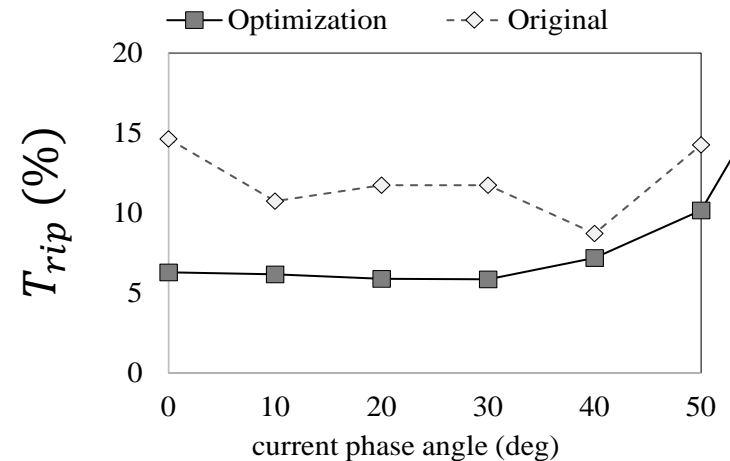
It is found from the measurement that the torque ripple is suppressed while the average torque is kept almost unchanged.



$$T_{rip} = \frac{T_{max} - T_{min}}{T_{average}}$$

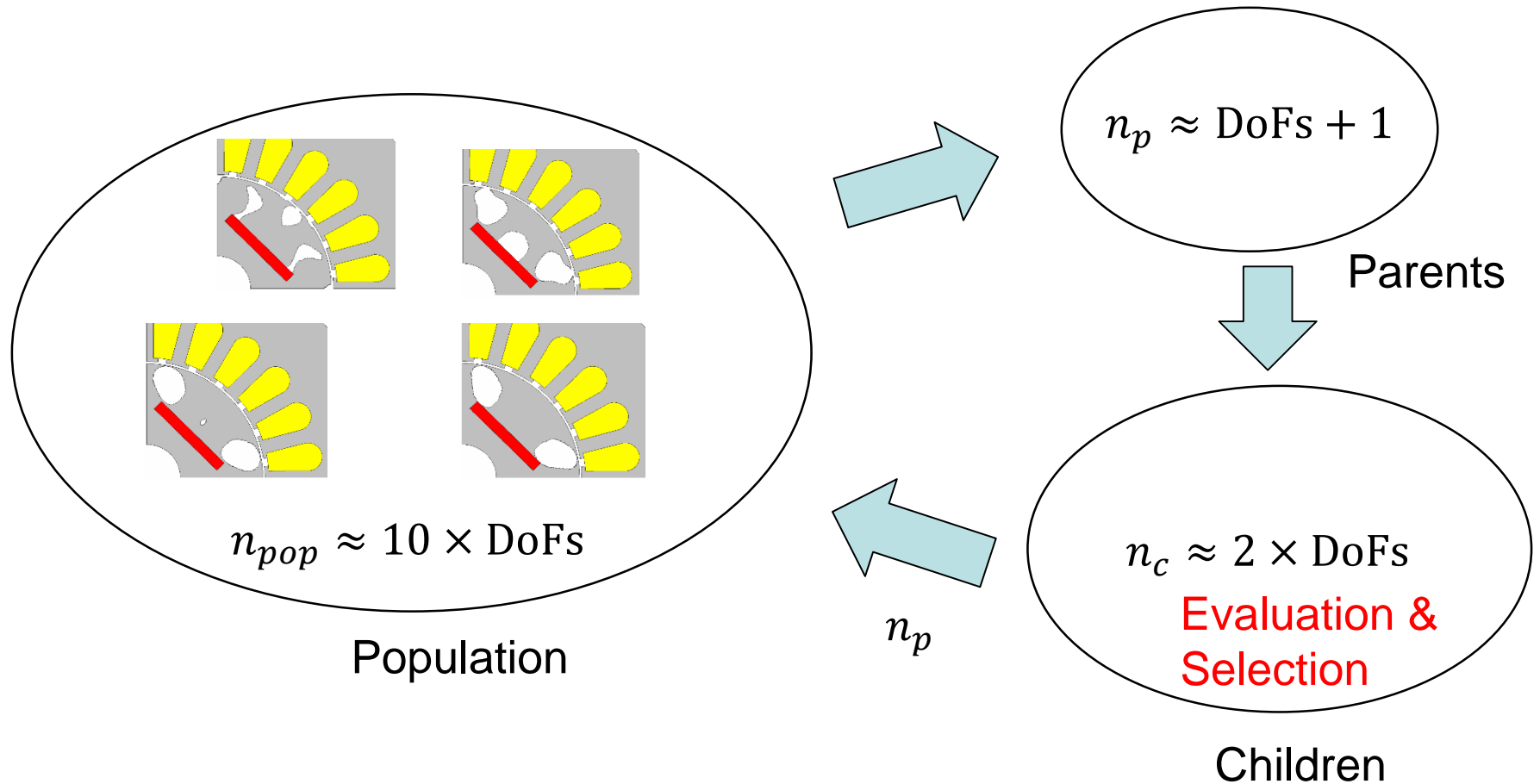


(a) Computed



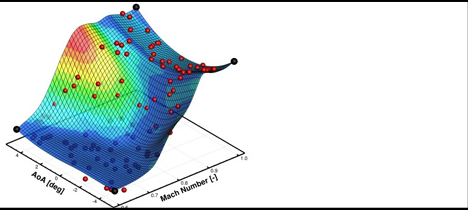
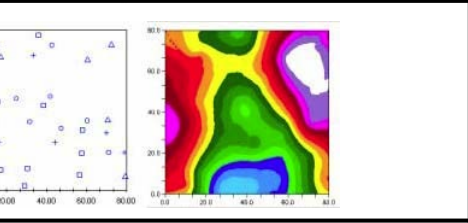
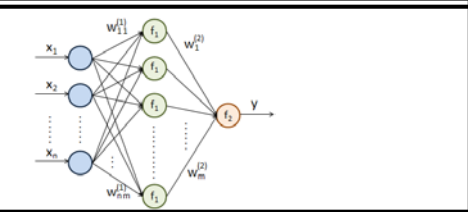
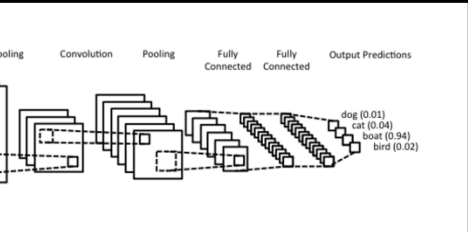
(b) Measured

# Real-coded Genetic Algorithm (with REX)



Finite element analysis has to be performed for  $2 \times \text{DoFs}$  times a generation.

# Surrogate Models (代理モデル)

| Methods  | Features   |
|--|--|
| <p>Response surface<br/>(応答曲面法)</p>  | <p>☹️ They do not work well for high-dimensional Problems.</p>   |
| <p>Kiriging</p>                      | <p>自由度が大きくなるとほぼ使えない</p>  |
| <p>Neural network</p>               | <p>☹️ Feature engineering is necessary.<br/>特徴量の定義が<b>必要</b></p> |
| <p>Deep Learning</p>               | <p>😊 Feature is automatically obtained.<br/>特徴量の定義が<b>不要</b></p> |

## GoogLeNet<sup>\*\*\*</sup>

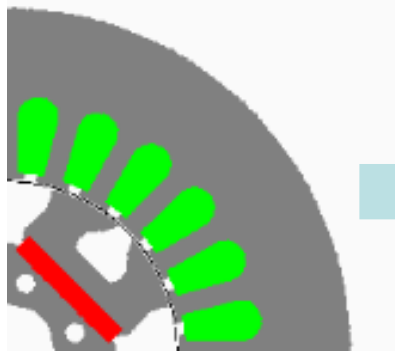
Convolutional neural network developed by Google.  
This outperforms the conventional machine learning methods.

### Classifier(分類器)

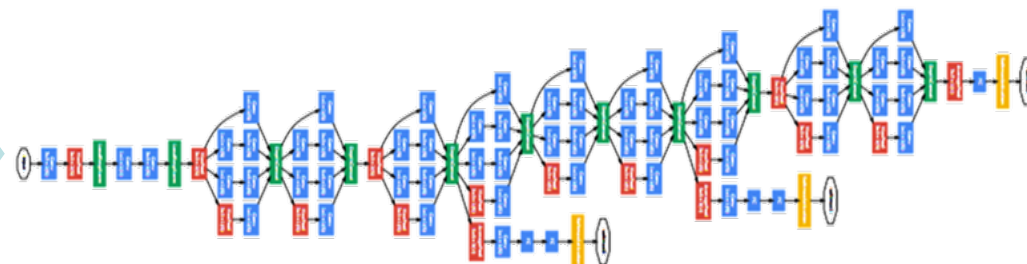
The IPM motors with different shapes are classified with respect to the average torque  $T_{ave}$  and torque ripple  $T_{rip}$ .

Input:

image of motor



Classifier



GoogLeNet \*

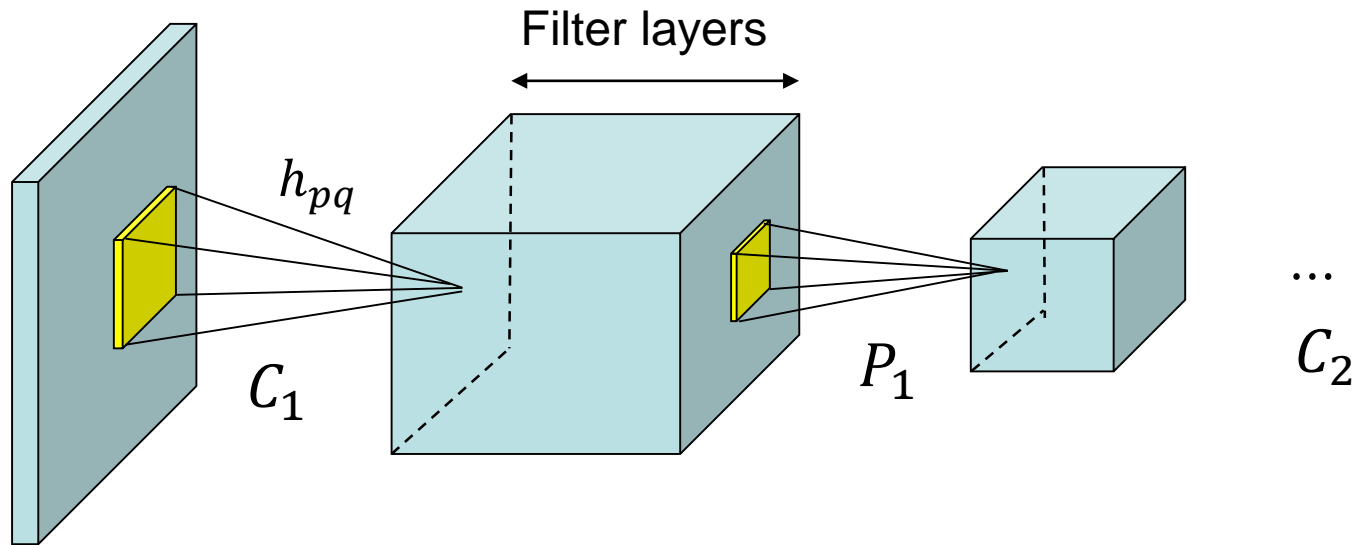
Output

$T_{ave}$

$T_{rip}$

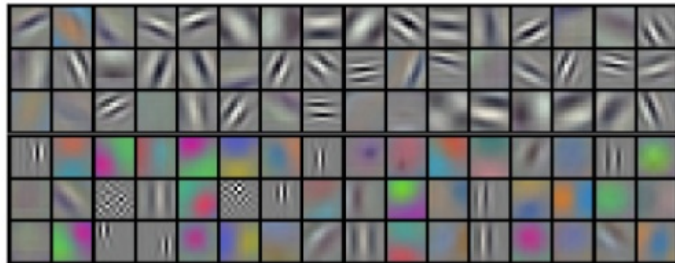
\*Szegedy, Christian, et al. "Going deeper with convolutions." Proceedings of the IEEE conference on computer vision and pattern recognition. 2015.

# Convolutional Neural Network (CNN)



$$x_{ij} = \sum_{p,q} y_{i+p,j+q} h_{pq} + b$$

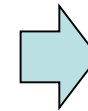
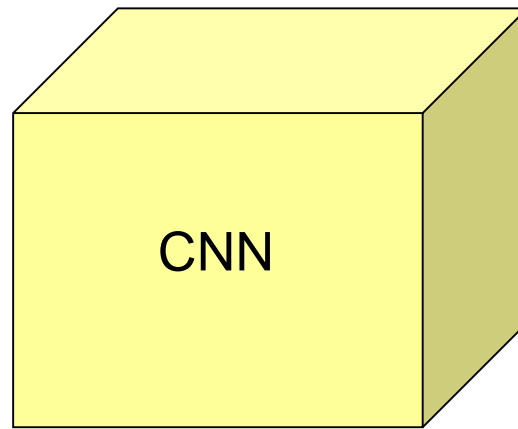
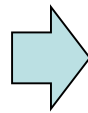
$$x_{ij} = \max_{p,q \in P_{ij}} y_{pq}$$



# Deep Learning for Image Recognition

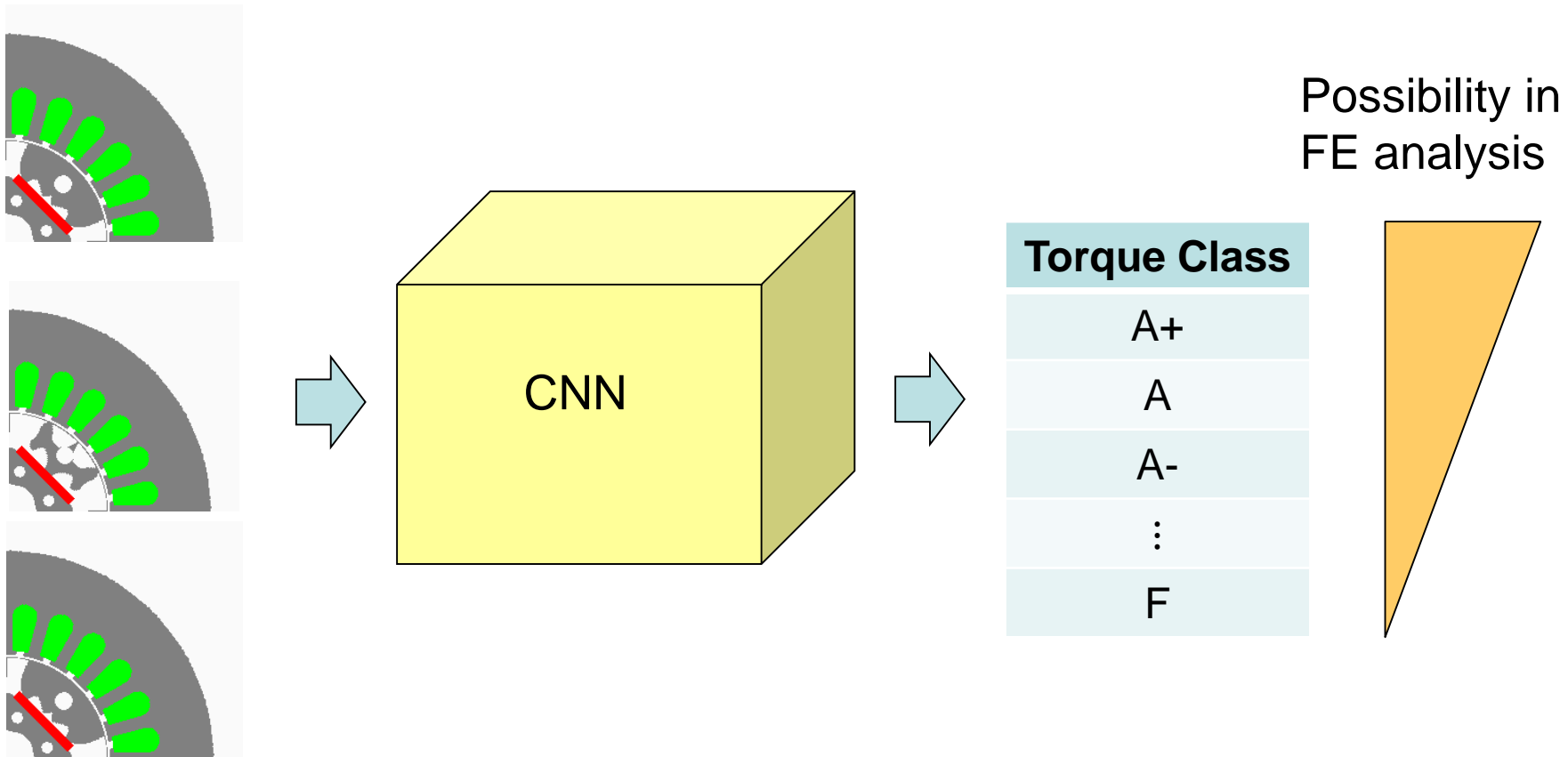


Internet



| class |
|-------|
| dog   |
| wolf  |
| fox   |
| ⋮     |

# Deep Learning for Topology Optimization



Topology optimization

# Generation of Data for DL with Topology Opt.

## Training phase

Training of CNN with the result for optimization **problem A**.

Training of CNN with the result for optimization with **small** number of individuals.

Training of CNN. Optimization problems are generated for **generalization of CNN**.

## Optimization phase

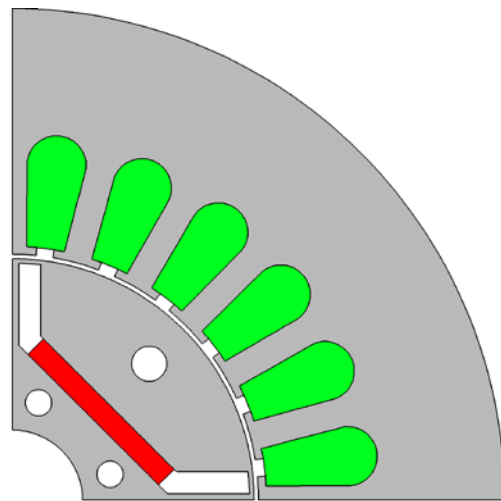
Optimization for different **problems B, C, D...** with CNN.

Optimization with **large** number of individuals with CNN.

Optimization with CNN for **wide class** of motors and problems.

Because the classification done by CNN is not perfect, **posterior FE analysis** is necessary for accurate evaluation. FE analysis is performed at high possibility for individuals in good classes.

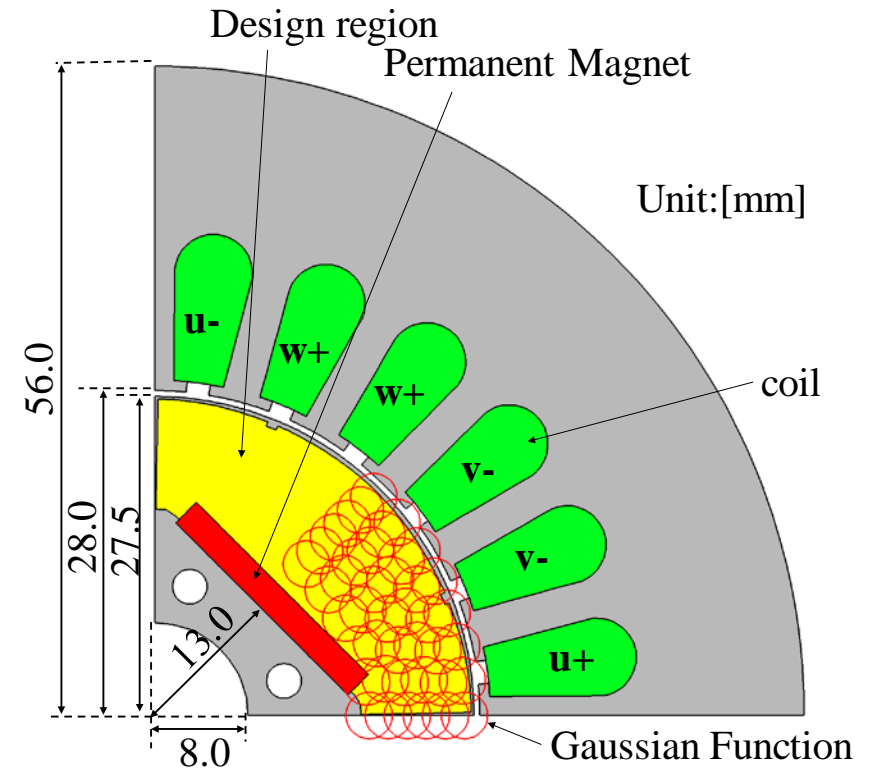
# Optimization of IPM motor



$$T^0 = 2.08 \text{ Nm}$$

$$T^0_{rip} = 0.57$$

|                              |        |
|------------------------------|--------|
| Current phase angle [degree] | 30     |
| Current effective value [A]  | 4.2425 |
| Number of turns [turn]       | 35     |
| Residual flux density [T]    | 1.25   |



[4] Technical report of the institute of electrical engineering of Japan,” *Industry application society*, No. 776, 2000.

# Optimization Problem

$$F = \frac{T}{T^0} \rightarrow \max.$$

$$\text{Sub.to. } N_{\text{area}} < 2$$

$T$ : Average torque

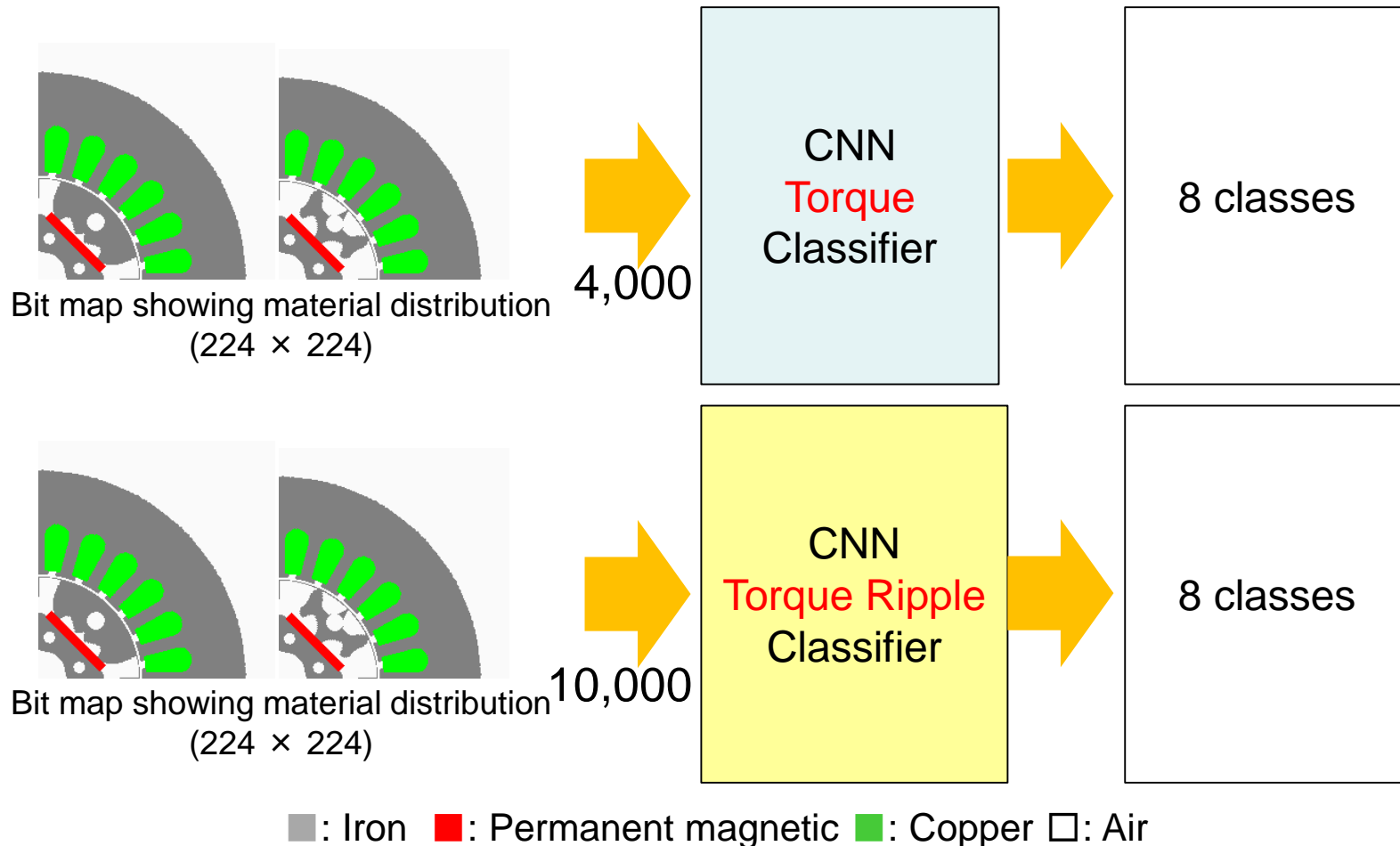
$T^0$ : Average torque of original model

$N_{\text{area}}$ : The number of separated rotor cores

## Optimization setting

|                           |     |
|---------------------------|-----|
| The number of genes       | 42  |
| The number of individuals | 800 |
| The number of children    | 160 |

# Training of CNN for classification of torque and torque ripple

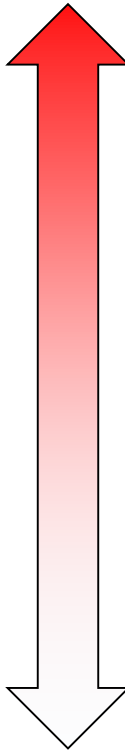


H. Sasaki, H. Igarashi, to be presented at CEFC2018 and submitted to IEEE Trans. Magn.

# Classification of torque and torque ripple

| Classification of Torque |           |
|--------------------------|-----------|
| CNN                      | FEM       |
| 1.1                      | 1.05~     |
| 1.0                      | 0.95~1.05 |
| 0.9                      | 0.85~0.95 |
| 0.8                      | 0.75~0.85 |
| 0.7                      | 0.65~0.75 |
| 0.6                      | 0.55~0.65 |
| 0.5                      | 0.45~0.55 |
| 0.0                      | ~0.45     |

better



worse

| Classification of Ripple |           |
|--------------------------|-----------|
| CNN                      | FEM       |
| 0.6                      | ~0.65     |
| 0.7                      | 0.65~0.75 |
| 0.8                      | 0.75~0.85 |
| 0.9                      | 0.85~0.95 |
| 1.0                      | 0.95~1.05 |
| 1.1                      | 1.05~1.15 |
| 1.2                      | 1.15~1.25 |
| 1.3                      | 1.25~     |

## Accuracy in torque

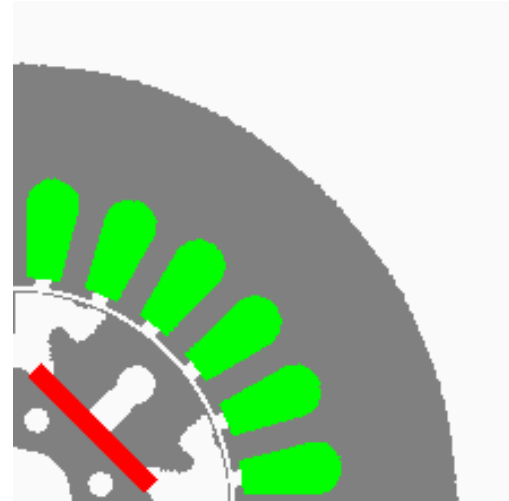
|                                    |              | Label by CNN $\hat{T}_{ave}^{CNN}$ |            |            |            |            |            |            |            | <b>TOTAL</b> |
|------------------------------------|--------------|------------------------------------|------------|------------|------------|------------|------------|------------|------------|--------------|
|                                    |              | 0                                  | 0.5        | 0.6        | 0.7        | 0.8        | 0.9        | 1          | 1.1        |              |
| Label by FEM $\hat{T}_{ave}^{FEM}$ | 0            | <b>513</b>                         | 46         | 10         | 6          | 2          | 7          | 0          | 0          | 584          |
|                                    | 0.5          | 18                                 | <b>397</b> | 75         | 1          | 0          | 0          | 0          | 0          | 491          |
|                                    | 0.6          | 0                                  | 83         | <b>392</b> | 79         | 0          | 0          | 0          | 0          | 554          |
|                                    | 0.7          | 0                                  | 1          | 73         | <b>462</b> | 39         | 1          | 0          | 0          | 576          |
|                                    | 0.8          | 0                                  | 0          | 0          | 32         | <b>377</b> | 29         | 0          | 0          | 438          |
|                                    | 0.9          | 0                                  | 0          | 0          | 6          | 40         | <b>463</b> | 28         | 0          | 537          |
|                                    | 1            | 0                                  | 0          | 0          | 0          | 0          | 21         | <b>368</b> | 26         | 415          |
|                                    | 1.1          | 0                                  | 0          | 0          | 0          | 0          | 0          | 10         | <b>395</b> | 405          |
|                                    | <b>TOTAL</b> | 531                                | 527        | 550        | 586        | 458        | 521        | 406        | 421        | 4000         |

H. Sasaki, H. Igarashi, to be presented at CEFC2018 and submitted to IEEE Trans. Magn.

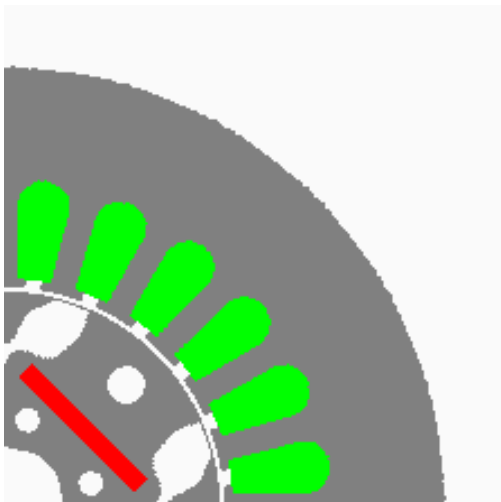
# Examples



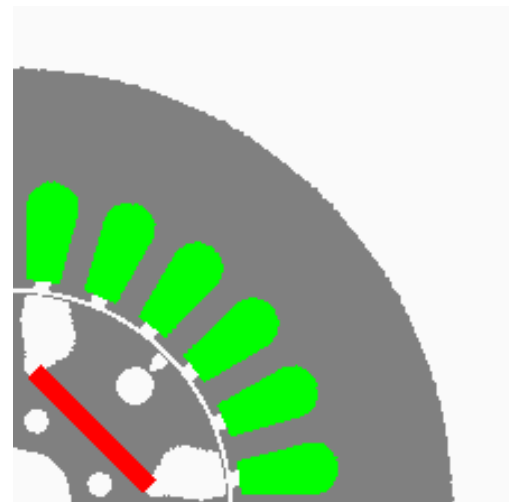
CNN: 0.50 FEM: 0.50



CNN: 0.90 FEM: 0.90



CNN: 0.70 FEM: 0.70



CNN: 1.10 FEM: 1.09

## Torque ripple

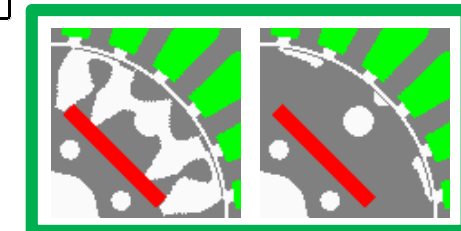
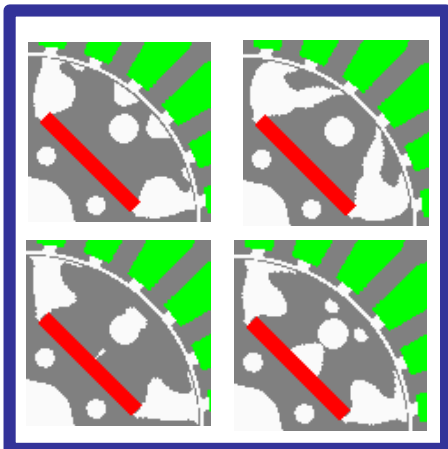
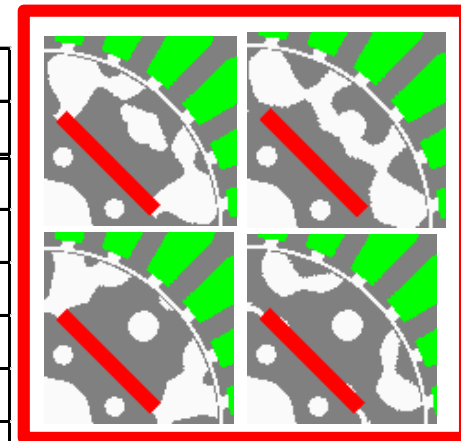
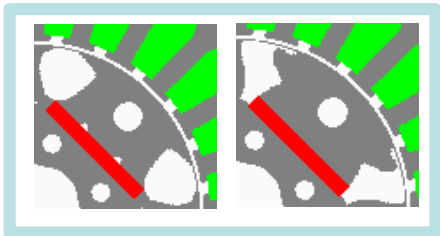
|  |       | Label by CNN $\hat{T}_{\text{rip}}^{\text{CNN}}$ |      |      |      |      |      |      |      |       |
|--|-------|--|------|------|------|------|------|------|------|-------|
|  |       | 0.6  | 0.7  | 0.8  | 0.9  | 1    | 1.1  | 1.2  | 1.3  | TOTAL |
| Label by FEM $\hat{T}_{\text{rip}}^{\text{FEM}}$ | 0.6   | 797  | 246  | 36   | 1    | 11   | 10   | 12   | 19   | 1132  |
|  | 0.7   | 169  | 631  | 164  | 99   | 20   | 33   | 21   | 29   | 1166  |
|  | 0.8   | 21   | 200  | 858  | 128  | 37   | 24   | 16   | 18   | 1302  |
|  | 0.9   | 7  | 114  | 139  | 812  | 122  | 136  | 41   | 12   | 1383  |
|  | 1     | 8  | 27   | 44   | 148  | 821  | 125  | 61   | 15   | 1249  |
|  | 1.1   | 5  | 36   | 29   | 115  | 108  | 850  | 250  | 27   | 1420  |
|  | 1.2   | 9  | 20   | 37   | 38   | 64   | 295  | 575  | 107  | 1145  |
|  | 1.3   | 21   | 19   | 32   | 26   | 33   | 36   | 240  | 796  | 1203  |
|  | TOTAL | 1037   | 1293 | 1339 | 1367 | 1216 | 1509 | 1216 | 1023 | 10000 |

H. Sasaki, H. Igarashi, to be presented at CEFC2018 and submitted to IEEE Trans. Magn.

# Torque ripple

Relationship between evaluation value by CNN and FEM

|                                    |       | Label by CNN $\hat{T}_{rip}^{CNN}$ |      |      |      |      |      |      |      | TOTAL |
|------------------------------------|-------|------------------------------------|------|------|------|------|------|------|------|-------|
|                                    |       | 0.6                                | 0.7  | 0.8  | 0.9  | 1    | 1.1  | 1.2  | 1.3  |       |
| Label by FEM $\hat{T}_{rip}^{FEM}$ | 0.6   | 797                                | 246  | 36   | 1    | 11   | 10   | 12   | 19   | 1132  |
|                                    | 0.7   | 169                                | 631  | 164  | 99   | 20   | 33   | 21   | 29   | 1166  |
|                                    | 0.8   | 21                                 | 200  | 858  | 128  | 37   | 24   | 16   | 18   | 1302  |
|                                    | 0.9   | 7                                  | 114  | 139  | 812  | 122  | 136  | 41   | 12   | 1383  |
|                                    | 1     | 8                                  | 27   | 44   | 148  | 821  | 125  | 61   | 15   | 1249  |
|                                    | 1.1   | 5                                  | 36   | 29   | 115  | 108  | 850  | 250  | 27   | 1420  |
|                                    | 1.2   | 9                                  | 20   | 37   | 38   | 64   | 295  | 575  | 107  | 1145  |
|                                    | 1.3   | 21                                 | 19   | 32   | 26   | 33   | 36   | 240  | 796  | 1203  |
|                                    | TOTAL | 1037                               | 1293 | 1339 | 1367 | 1216 | 1509 | 1216 | 1023 | 10000 |

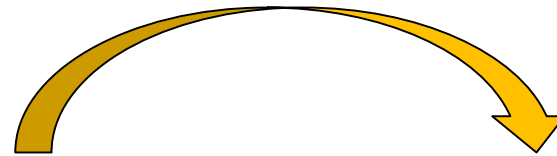


## Coevolution in biology

Wiki: In biology, **coevolution** occurs when two or more species reciprocally affect each other's evolution.

## Toward Coevolution of DL and TO

Fitness evaluation



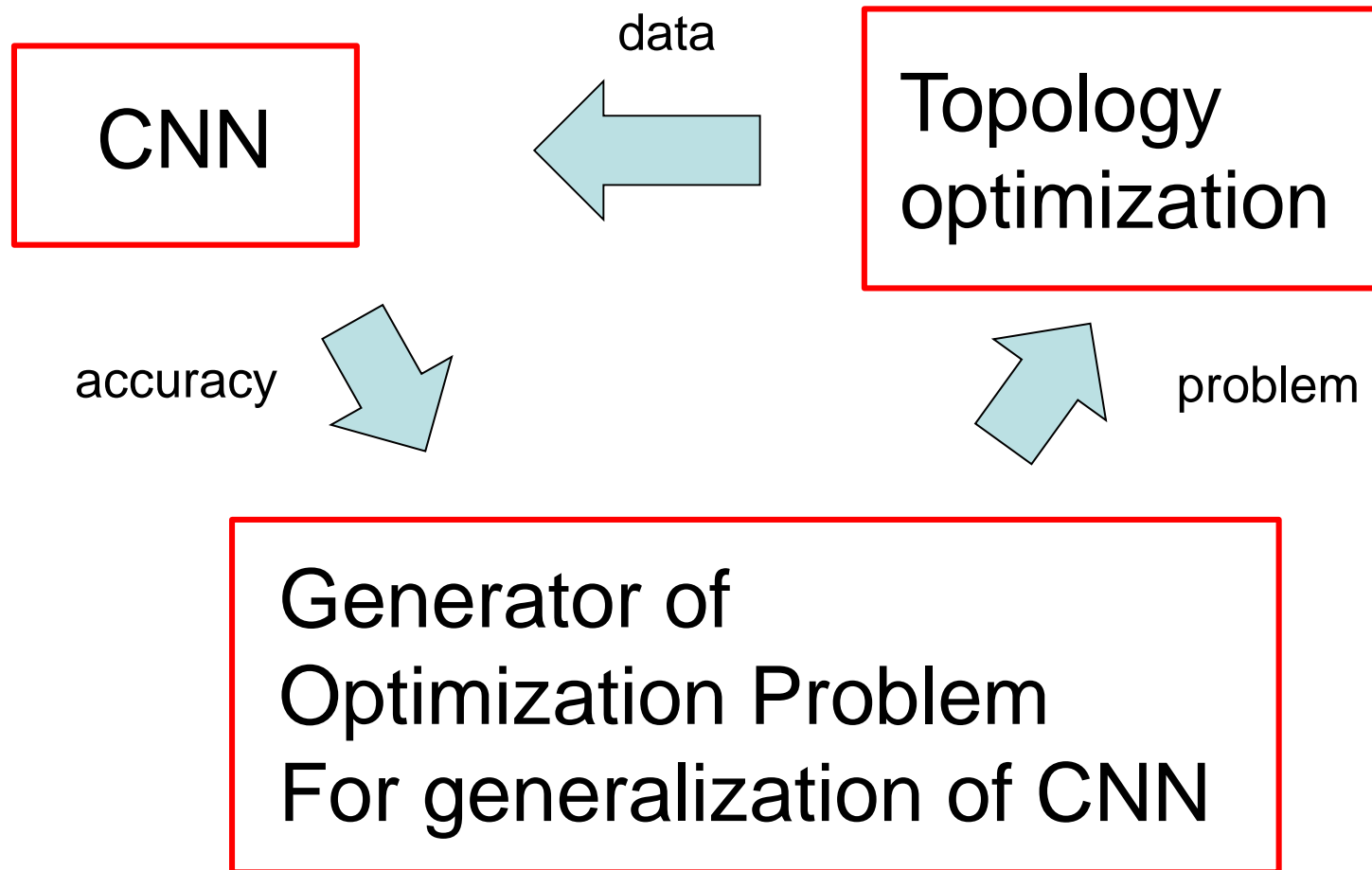
Training of CNN  
with richer data

Topology optimization  
with faster speed



Training data

# Building a Strong Classifier with DL



# Conclusions

Topology optimization leads to new design to various electric and electronic apparatus as well as other mechanical and chemical Systems.

Deep learning is promising to reduce the computational cost of Topology optimization.

Topology optimization and deep learning can make coevolution. Using the topology optimization, we would be able to realize *a strong classifier with generality* of electric motors as well as other devices.

